INFORMATION TO USERS

This dissertation was produced from a microfilm copy of the original document. While the most advanced technological means to photograph and reproduce this document have been used, the quality is heavily dependent upon the quality of the original submitted.

The following explanation of techniques is provided to help you understand markings or patterns which may appear on this reproduction.

1. The sign or "target" for pages apparently lacking from the document photographed is "Missing Page(s)". If it was possible to obtain the missing page(s) or section, they are spliced into the film along with adjacent pages. This may have necessitated cutting thru an image and duplicating adjacent pages to insure you complete continuity.

2. When an image on the film is obliterated with a large round black mark, it is an indication that the photographer suspected that the copy may have moved during exposure and thus cause a blurred image. You will find a good image of the page in the adjacent frame.

3. When a map, drawing or chart, etc., was part of the material being photographed the photographer followed a definite method in "sectioning" the material. It is customary to begin photoing at the upper left hand corner of a large sheet and to continue photoing from left to right in equal sections with a small overlap. If necessary, sectioning is continued again — beginning below the first row and continuing on until complete.

4. The majority of users indicate that the textual content is of greatest value, however, a somewhat higher quality reproduction could be made from "photographs" if essential to the understanding of the dissertation. Silver prints of "photographs" may be ordered at additional charge by writing the Order Department, giving the catalog number, title, author and specific pages you wish reproduced.

University Microfilms

300 North Zeeb Road
Ann Arbor, Michigan 48106

A Xerox Education Company

PROPERTIES OF UNIDIRECTIONALLY SOLIDIFIED ALLOYS

by

Edward Benn

A Dissertation Submitted to the Faculty of the

DEPARTMENT OF METALLURGICAL ENGINEERING

In Partial Fulfillment of the Requirements
For the Degree of

DOCTOR OF PHILOSOPHY
WITH A MAJOR IN METALLURGY

In the Graduate College

THE UNIVERSITY OF ARIZONA

1 9 7 2

THE UNIVERSITY OF ARIZONA

GRADUATE COLLEGE

I hereby recommend that this dissertation prepared under my direction by Edward Benn entitled Properties of Unidirectionally Solidified Alloys be accepted as fulfilling the dissertation requirement of the degree of Doctor of Philosophy

Walter W. Walker — June 13, 1972
Dissertation Director — Date

After inspection of the final copy of the dissertation, the following members of the Final Examination Committee concur in its approval and recommend its acceptance:*

Walter W. Walker	June 13, 1972
Louis J. Demer	June 13, 1972
Alan J. Milne	June 13, 1972
Paul A. Pickard	June 30, 1972
[illegible]	July 3, 1972

*This approval and acceptance is contingent on the candidate's adequate performance and defense of this dissertation at the final oral examination. The inclusion of this sheet bound into the library copy of the dissertation is evidence of satisfactory performance at the final examination.

STATEMENT BY AUTHOR

This dissertation has been submitted in partial fulfillment of the requirements for an advanced degree at The University of Arizona and is deposited in the University Library to be made available to borrowers under rules of the Library.

Brief quotations from this dissertation are allowable without special permission, provided that accurate acknowledgment of source is made. Requests for permission for extended quotation from or reproduction of this manuscript in whole or in part may be granted by the head of the major department or the Dean of the Graduate College when in his judgment the proposed use of the material is in the interests of scholarship. In all other instances, however, permission must be obtained from the author.

SIGNED: Edward C Bass

ACKNOWLEDGMENTS

The author would like to thank the many people on the staff of the Optical Sciences Center who assisted in making this document possible. Particular gratitude is extended to George Kew for photography, the optics shop, electronics shop and the machine shop.

During the periods of experimenting, I was ably assisted by Mr. Larry Andre whose experience in precision casting was appreciably utilized. My research was guided by the insight of my adviser, Dr. W. W. Walker of Metallurgical Engineering. Also, a special note of thanks for Dr. L. J. Demer for his advice on the interpretation of the results and his literary criticism.

This research was sponsored by the U. S. Air Force THEMIS program under contract No. F0-4695-67-C-0197.

TABLE OF CONTENTS

LIST OF ILLUSTRATIONS

LIST OF ILLUSTRATIONS--Continued

LIST OF ILLUSTRATIONS--Continued

LIST OF ILLUSTRATIONS--Continued

LIST OF ILLUSTRATIONS--Continued

LIST OF TABLES

ABSTRACT

The properties of unidirectionally solidified (UDS) aluminum alloys were investigated metallographically, mechanically, and dimensionally. Three distinct structures were obtained and tested: random polycrystals, columnar crystals, and growth twin or "feather" crystals. In two-phase alloys, samples containing columnar and feather crystals showed a marked increase in mechanical properties over randomly structured samples in the as-cast condition.

Experiments were performed to determine the nature and conditions of nucleation for feather crystals. The effects of increasing solute content in unidirectionally cast Al-Cu alloys were observed. It was also observed that feather crystals only occur over a limited range of solute concentration.

Several commercial aluminum casting alloys were investigated for use as substrates of optical mirrors. Both conventional and UDS (longitudinal and transverse) castings were examined for grain structure and polished to an optically flat surface. Interferometer readings were made on these surfaces before and after thermal cycling from -80 to 160°F. Castings containing grains with directional structures showed an improved dimensional stability when compared to castings containing random polycrystals.

Explanations of the data are presented in terms of fiber strengthening, interdendritic eutectic distribution, and microyielding.

INTRODUCTION

The past decade has seen a revolutionary advancement in the art of metal founding. Methods of modern technology have been introduced to an art that is nearly 5000 years old. Not only does the modern engineer have a myriad of metallic materials to choose from, but he can also design for casting complex structures to precision tolerances thus avoiding the necessity of expensive metal shaping and removal processes.

Castings of aluminum alloys are traditionally believed to have a 50% lower tensile strength than wrought alloys of similar composition. This is attributed to the typical microshrinkage and gas porosity resulting from normal foundry practices. There are many non-critical applications for these materials, and their lack of strength is compensated for by increasing the physical size of the casting. In modern foundry practices, by careful control of solidification, castings can be obtained with much improved properties.

Directional casting is a simplified method of producing a material similar to a fiber reinforced composite. A composite is usually made by arranging fibers of a high strength brittle material in the form of parallel plates or rods in a mold cavity, then filling the mold with a matrix of a compatible plastic material. The result, ideally, is a material with strength and ductility contributed by both

components. Although materials of this type have been successfully utilized (fiberglass), the cost of producing complex shapes is far greater than that for direct casting.

If a metal could be cast directly from a melt and show the structure and properties of a composite material, then foundry products would be more competitive with wrought products. Very little data have been made available on the properties improved by unidirectional solidification and a correlation of directional structures with these properties has never been investigated in detail. Since the principal interest of my sponsors (THEMIS) was materials for lightweight mirrors, an excellent opportunity to conduct unidirectional solidification research was made available.

Of particular interest in the investigation was the occurrence of growth twin (feather) crystals in unidirectionally solidified aluminum alloys. The morphology and properties of this structure were compared to columnar and random structures obtained in the same alloys. The results of this investigation are the basis of this dissertation.

THEORY OF SOLIDIFICATION

Kinetics

The solidification of metals has been the subject of a great deal of scientific investigation during this century. Much of the early theory was presented by Tammann (1925). Many of his observations have been verified while others have been modified by the knowledge of interatomic forces and other solid state considerations which have been discovered since his time. Early concepts of solidification were simply based on heterogeneous nucleation and the growth of dendrites. In a review of the subject, Doan (1953) pointed out that most original work was in nucleation. In the present investigation, nucleation was not controlled and will not be discussed at length.

In analyzing the growth of crystals from the melt, it is convenient to consider unidirectional heat removal as the main driving force for solidification. By doing so, the mathematical modeling is simplified to a two-dimensional or planar problem. As a basic approach, consider a solid-liquid interface in a bar of unidirectionally solidifying metal. At the interface, a continuous process of melting and freezing as competing phenomena is occurring (Chalmers, 1954; Elbaum and Chalmers, 1955). The rates of these processes can be represented kinetically by the following expressions where the subscripts f and m stand for freezing and melting.

$$R_f = A_f G_f v \exp(-Q_f/kT)$$

$$R_m = A_m G_m v \exp(-Q_m/kT)$$

where:

R = rate in cm/sec or in/sec

A = atomic accomodation coefficient

G = probability that vibration is toward the interface

v = atomic vibration frequency in Hz

Q = average energy of the atoms

k = Boltzmann constant

T = absolute temperature at the interface in °K.

The atomic accomodation coefficient for freezing, A_f, represents the probability that a metal atom moving from the liquid to the interface will find a place to adhere and become part of the solid. This is directly related to the crystallography of the solid metal. In face-centered metals such as aluminum and copper, the {111} type of interface has the lowest accomodation coefficient. The value of A_m is the same for all monatomic liquids.

At equilibrium, the two competing rates are equal and there is no growth. The accomodation coefficients are related at this point by:

$$\ln(A_f/A_m) = L/kT_{eq}$$

where L is the latent heat of fusion in cal/gram and T_{eq} is the temperature of the solid-liquid interface at equilibrium.

This theoretical approach to solidification does not correspond to the observed requirement of supercooling as a prerequisite for solidification. Although the quantities A_f and A_m are related in terms of the latent heat of fusion, the equations do not explain the degree of supercooling which occurs without solidification in ultrapure metals. A more pragmatic approach has been presented by several investigators.

Pure Metals

In a pure metal, the projection of the solid interface into the melt depends on the temperature rise in the liquid ahead of the interface. From the preceding discussion on accomodation coefficients, it would appear that a controlled growth would have a preferred structure. In pure metals, quite often the {111} and {100} faces are parallel to the growth interface when the solidification is very slow. However, when solidified at faster rates, liquid motion causes the structure to become more random.

In a more recent fundamental discussion (Winegard, 1964), a macroview of solidification was presented. In this approach, an advancing solid interface is analyzed in terms of possible thermal gradients as shown in Fig. 1.

With a positive temperature gradient in the liquid, no growth of the interface will occur (Jackson and Chalmers, 1956). This condition is analogous to $R_f = R_m$ in the atomic solidification model previously described. In order for the solid to advance into the liquid, some supercooling must exist.

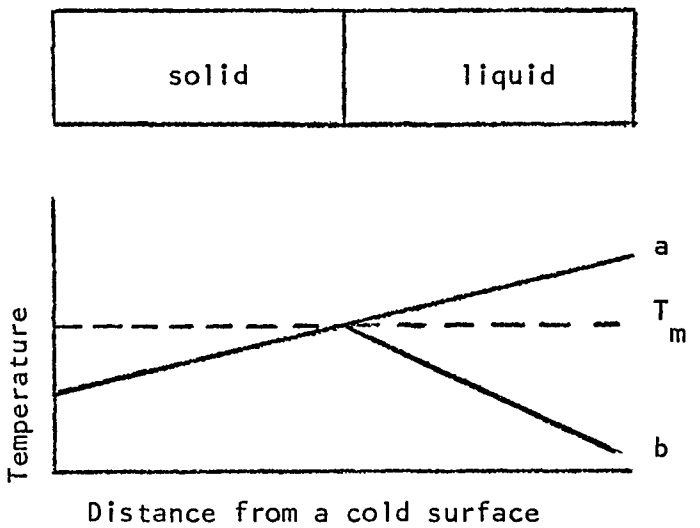

Fig. 1. Temperature-Distance Relations in Unidirectional Solidification.

a. Positive liquid temperature gradient
b. Negative liquid temperature gradient

When a very small degree of supercooling is employed, the solid-liquid interface exposed by decanting shows a terraced or platelet-like structure (Graf, 1954; Rosenberg, 1956). The platelets were found to be parallel to close-packed planes in FCC metals and had a preferred orientation (Rosenberg and Tiller, 1957) as shown in Fig. 2.

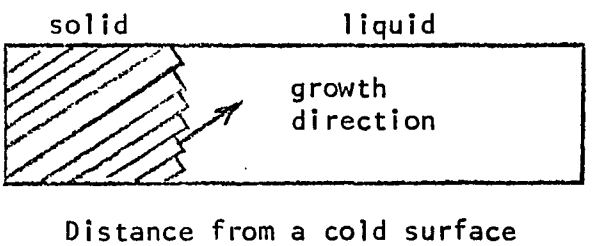

Fig. 2. Platelet Growth in Pure Metals.

If the temperature gradient is negative in the liquid (curve b, Fig. 1), then the liquid is supercooled and solid growth is dendritic in nature. The shape of curve b, which illustrates a temperature inversion, seems to violate the second law of thermodynamics. A more acceptable model would show that the latent heat of fusion is rejected into the liquid to maintain a positive temperature gradient adjacent to the solid interface. The growth direction of dendrites in FCC metals is <100>, (Wineberg and Chalmers, 1951).

The degree of supercooling influences both the growth rate of the solid into the liquid and the spacing of the dendrite stalks as shown in Fig. 3 and Fig. 4.

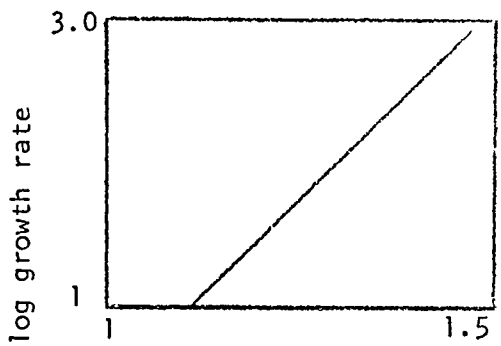

Fig. 3. Dendrite Growth Rate as a Function of Supercooling

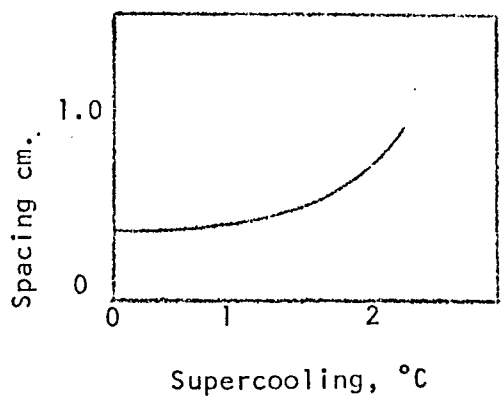

Fig. 4. Dendrite Spacing as a Function of Supercooling

The phenomenon of chill casting and its resulting structures are most vividly displayed in metal ingots. In this situation a metal is superheated to a temperature far above its melting temperature and poured into mold. The mold is usually made of a high melting temperature, high conductivity material such as steel for molten aluminum. Solidification proceeds by copious nucleation on the cold mold walls thus creating

a skin of very fine-grained crystals. In a small thickness of solid, the interface temperature equals the equilibrium melting temperature of the metal and nucleation of new grains ceases. This is due to the conduction of heat from the superheated melt to the mold through the skin metal. At this point, solidification proceeds under the conditions of Curve a, Fig. 1.

In pure metals, the degree of supercooling at the interface which is in thermal equilibrium with a superheated melt is sufficient for the growth of several existing skin grains. This amount of supercooling is inadequate for the nucleation of new grains as pointed out by Walker (1958) and shown schematically in Fig. 5.

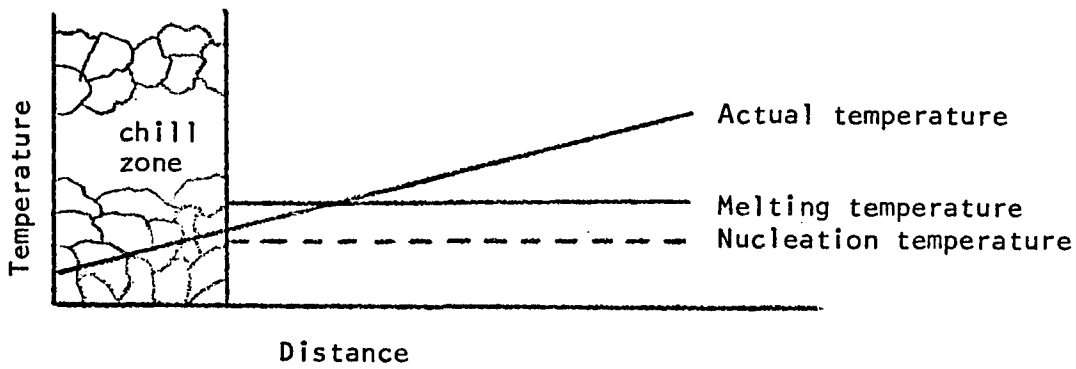

Fig. 5. Thermal Conditions During Freezing of a Pure Metal Ingot.

The resulting structure which grows from the fine-grained skin is that of long columnar crystals. The transition from the chilled zone to the columnar crystal zone in a pure metal ingot is shown in Fig. 6.

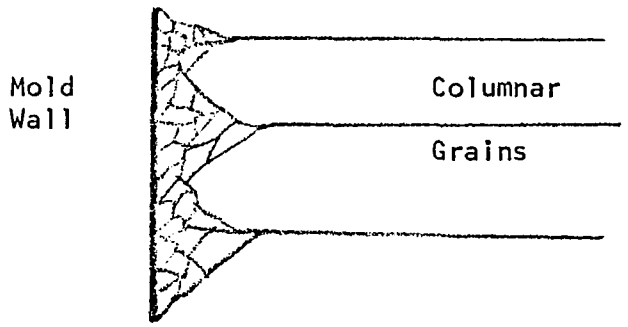

Fig. 6. Chill and Columnar Zones of an Ingot.

The surviving chill grains which make up the columns all have a "dendrite direction" perpendicular to the mold wall. However, the columnar crystals of a pure metal are not made up of dendrites since there is no supercooled liquid in a superheated melt. The "dendrite direction" growth rate of columnar crystals is most favorable due to the more efficient conduction of latent heat of fusion to the mold walls. These characteristics differ with the observations made in alloy solidification which will now be discussed.

Alloys

In pure metals, eutectics, and congruent melting intermetallic compounds, freezing occurs at a definite equilibrium temperature. In alloys or metals with impurities, liquid and solid can coexist over a range of temperatures.

As in pure metals, the rate of solidification in alloys is related to the degree of supercooling at the solid-liquid interface. In pure metals, supercooling is by thermal inversion to create a dendritic structure. In alloys, supercooling can be produced by both

changes in temperature and composition. This last phenomenon is called constitutional supercooling which is explained in the following discussion.

The terminal end of an alloy phase diagram is shown in Fig. 7. The solidification of an alloy of composition C_o occurs over the temperature range as shown. The distribution coefficient (k_o) is defined as the ratio of the solute concentration of the metal solidified at a specific temperature to the solute concentration of the liquid in equilibrium with it at the same temperature or $k_o = C_s/C_l$.

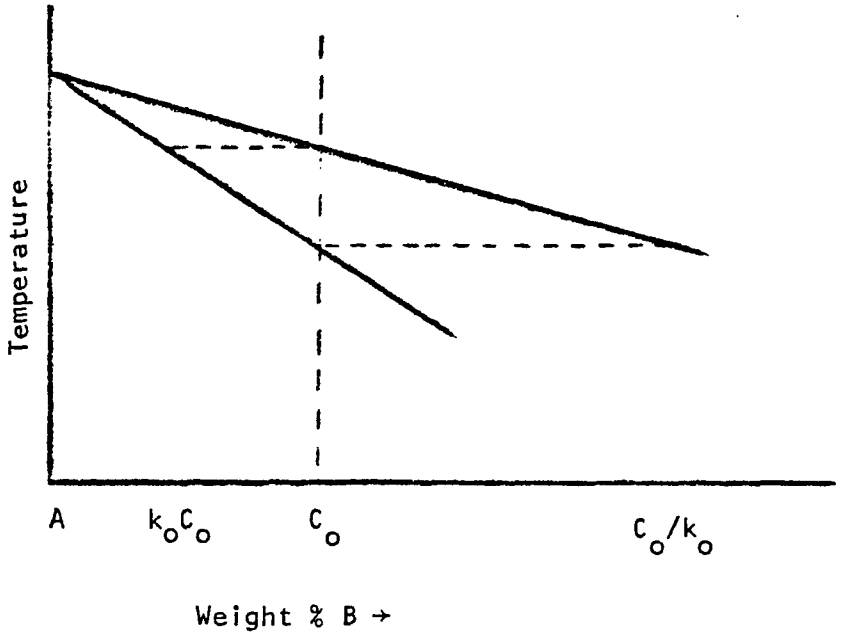

Fig. 7. Concentration Phase Diagram where $k_o < 1$.

The final structure of alloy C_o depends on both thermal and diffusion conditions. If we assume the following:

a. k_o is a constant.

b. Diffusion in the solid is negligible.

c. Diffusion is the only mechanism of mixing in the liquid.

d. Equilibrium is maintained at the solid-liquid interface, i.e., $C_s = k_o C_l$.

then the freezing procedure of C_o can be described. The general outline of the solidification can be postulated as:

a. The first solid formed is of composition $k_o C_o$ which indicates that solute is rejected.

b. The solute content of the liquid increases with decreasing temperature.

c. At a constant rate of growth, an equilibrium between solute rejection and solute diffusing from the interface into the liquid is established.

d. The last solid to form is C_o in solute.

e. The bulk concentration of the last liquid is C_o/k_o.

If we consider solidification to be unidirectional, a relationship between solute concentration in the liquid and the distance from the advancing solid-liquid interface can be shown. The equilibrium freezing temperature of the liquid can also be related to the same distance, as shown in Fig. 8.

In an idealized case, we can show the contrast between the growth of pure metals and alloys graphically. The relation between the actual temperature and the equilibrium freezing temperature in solidifying superheated pure metal and alloy ingots is shown in Fig. 9.

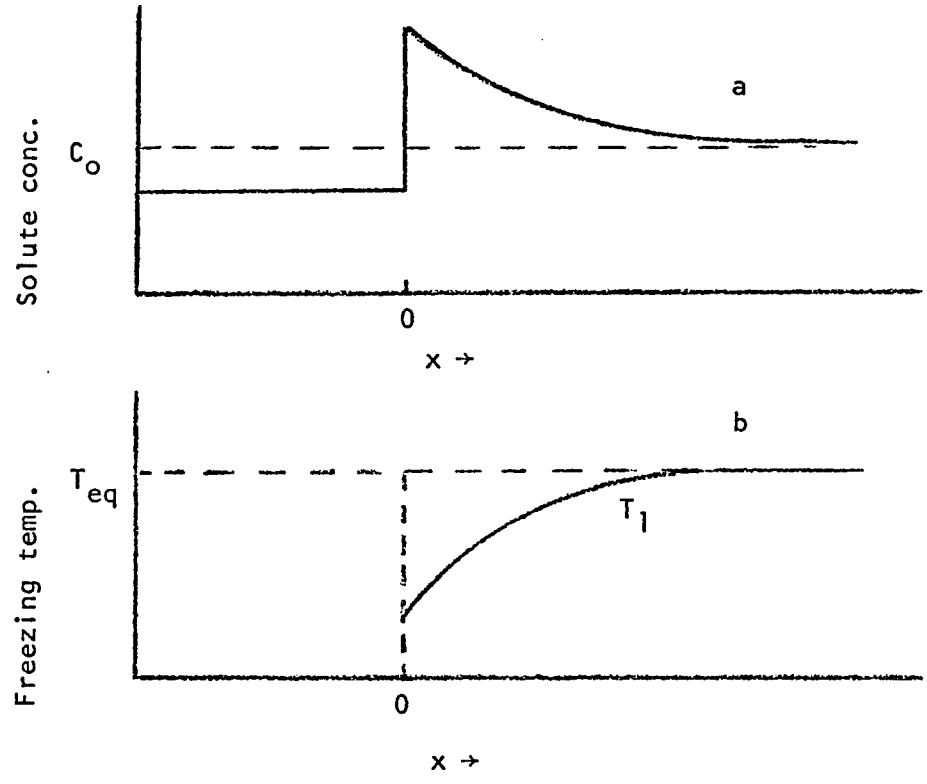

Fig. 8. Freezing Relationships at the Solid-Liquid Interface Due to Constitutional Supercooling.

a. Concentration gradient ahead of the interface.
b. Equilibrium freezing temperature of the liquid.
x = Distance away from the interface into the liquid.
T_l = The equilibrium freezing temperature of the liquid.

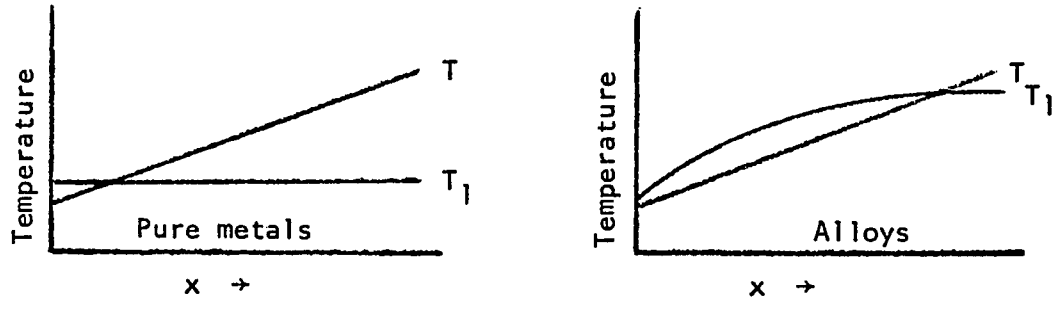

Fig. 9. Equilibrium Freezing Temperature vs. Actual Temperature for Pure Metals and Alloys.

Here we may see that the alloy has the ability to grow dendritically from the interface (x=0) due to constitutional supercooling.

It has been shown (Pfann, 1957) that as the solid layer increases in thickness, the value of the distribution coefficient departs from k_o. The new value, k, is called the effective distribution coefficient and may be approximated from the expression:

$$k/k_o = 1/(k_o + (1-k_o)\ \exp(-Rx/D))$$

where:

R = rate of solidification.

x = distance ahead of the solid-liquid interface into the liquid.

D = the diffusion coefficient of the solute in the liquid.

The composition of the liquid (C_l) at any distance ahead of the interface (x) may be calculated from:

$$C_l = C_o[1 + (1-k_o/k_o)\ \exp(-Rx/D)].$$

The equilibrium freezing temperature corresponding to this same distance and composition is given by:

$$T_l = T_o - mC_l$$

where m is the slope of the liquidus line and T_o is the freezing temperature of pure solvent.

Constitutional supercooling can be used to explain solute distribution and alloy structures obtained in unidirectional solidification. The typical solute distribution observed in alloy solidification is shown in Fig. 10 (Tiller, 1962).

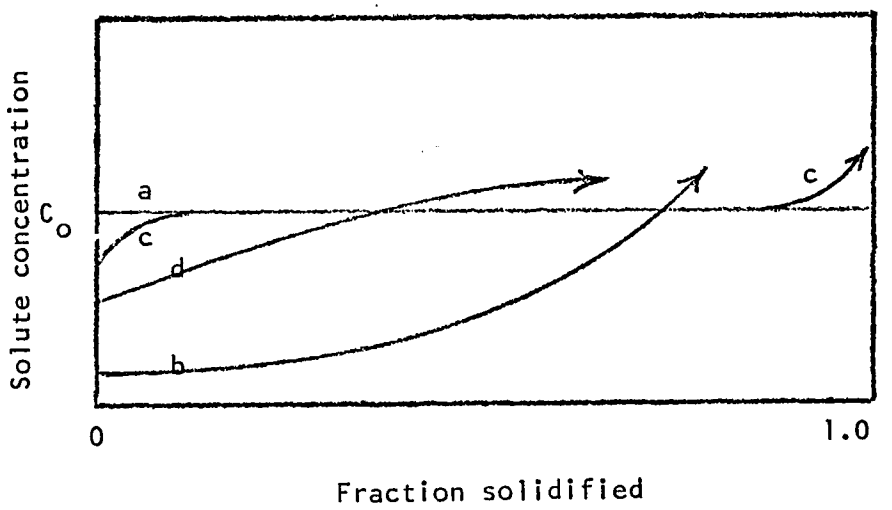

Fig. 10. Solute Distribution in a Unidirectionally Solidified Alloy of Initial Concentration C_o.

a. Complete diffusion in solid and liquid.
b. Complete mixing in liquid ($k=k_o$)
c. Mixing by diffusion in liquid only.
d. Partial mixing in liquid $k=(1+k_o)/2$

The freezing rates corresponding to the curves of Fig. 10 are increasing from a to c. Case d is the one most generally realized in practice as "normal freezing".

The forms of segregation encountered in alloy solidification are: banding, gravity segregation, interdendritic, intercellular and intergranular segregation. Particular interest will be directed to interdendritic segregation later in the review.

The type of grain structure obtained during the unidirectional solidification of alloys depends on the degree of constitutional supercooling and the solidification rate applied. Many investigators have analyzed the decanted solid-liquid interface as an approach to structure

prediction. The relationship between alloy solidification interface structure and the cooling parameter is shown in Fig. 11 (Hurle, 1962).

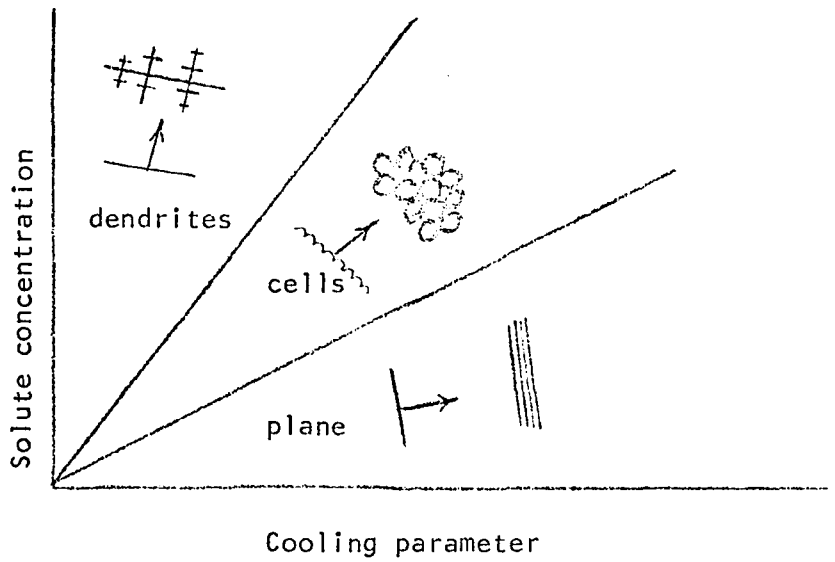

Fig. 11. Alloy structures and Interface Forms as a Function of Solute Concentration and Cooling Rate.

The cooling parameter of Fig. 11 has been subject to controversy during recent years. The most popular current value is given as $G/R^{1/2}$ (Plaskett and Winegard,1950) where G is the temperature gradient in the liquid ahead of the interface and R is the rate of solidification. The original parameter postulated (Rutter and Chalmers, 1953) was G/R.

It has been shown that when the temperature gradient is shallow, constitutional supercooling brings about instabilities in the solid interface. These surfaces, through a mechanism of lateral and forward solute rejection, form the structure of cells (Tiller and Rutter, 1956; Walton, Tiller, Rutter and Winegard, 1955).

The work of Plaskett and Winegard on aluminum-magnesium alloys showed the relationships between distance from a chill surface and the cooling parameters. These relationships are shown in Fig. 12.

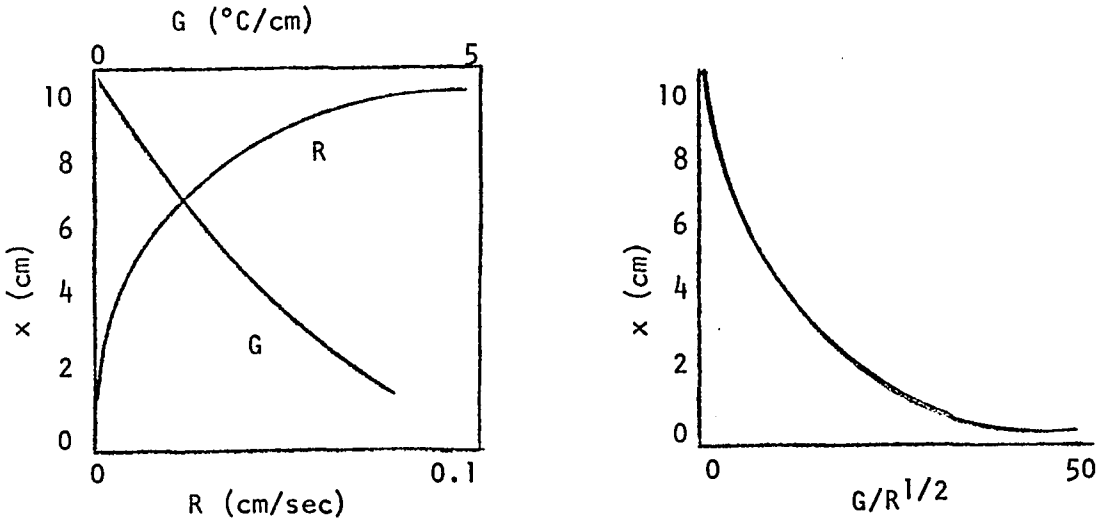

Fig. 12. Variation of the Parameters G and R with the Distance from a Chill Surface for Al-2 Mg Alloy.

These curves show the classical kinetic relationship of nucleation and growth. A very steep thermal gradient such as when a superheated melt is cast against a chill plate represents a fast growth rate. The data for Fig. 12 were obtained in an experiment where a melt was in equilibrium with a surface which was then chilled. The relationships shown in Fig. 12 apply to all chill casting techniques.

The theoretical approach to the solid-liquid interface morphology is complex. The structures are dependent on the temperature and solute concentration distributions along with several physical shape (curvature of the interface projections) and mechanical parameters. Equations have been written (Cahn, 1965) which define the growth rate of a surface whose

direction normal forms an angle with the primary crystallographic directions. Equations of this type are functions of atomic kinetic parameters and are spatially dependent.

Experimental observations in Sn-Pb alloys using controlled gradients and rapid anvil-type decantations have been made. The results showed that a number of interface forms can be created between the basic types shown in Fig. 11. All of these structures relate directly to the amount of constitutional supercooling and solute redistribution ahead of the solid interface.

An understanding of the interface variation between plane and cells can be visualized in Fig. 13.

What Fig. 13 shows is that when the thermal gradient is steep (G_o), no constitutional supercooling occurs. This situation is analogous to the growth of a pure metal with an uninverted temperature gradient. As the gradient becomes more horizontal, the interface becomes increasingly more segregated.

Unfortunately, all of the investigators in this field fail to draw any relationships between decantation interface structures and the macrostructures of cast ingots. Apparently, when the thermal gradient is steep enough to produce planar or even cellular interfaces, the ingot structures are generally randomly oriented polycrystals. Since the principal interest of this work is the properties of directional crystals, we shall now discuss columnar crystals in alloys.

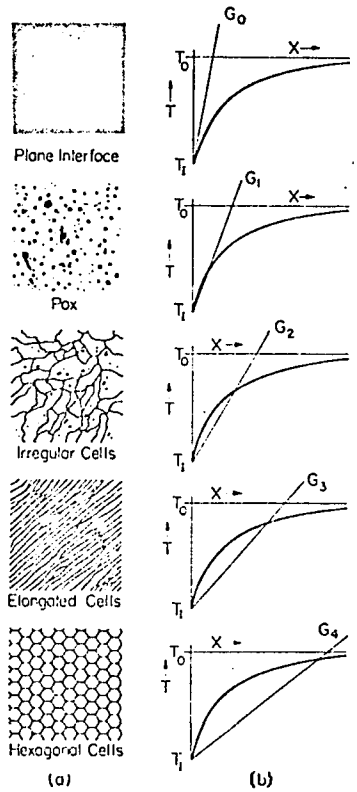

Fig. 13. Illustration Showing the Variation in Decanted Interface Structure with Constitutional Supercooling and Temperature Gradient.

(a) Interface appearance

(b) Equilibrium Freezing temperature and temperature gradient

Columnar Crystals

In alloys, columnar crystals are grown dendritically. One of the main characteristics of columnar crystals is that the long axes of growing dendrites are parallel to the direction of heat flow. In FCC metal, this is the <100> direction (Northcott, 1939). Usually, columnar grains are not desirable in commercial castings due to anisotropic

mechanical properties (Flemmings, Uram and Taylor, 1960). However, this anisotropy can be utilized in specific applications such as turbine blades (Piearcey and Versnyder, 1966) and perhaps in astronomical mirrors (Benn and Walker, 1971).

During directional solidification, the temperature gradient at the solid-liquid interface changes as the solid thickness increases. Also the generation of crystal nuclei is related to the distance from the chill surface, degree of supercooling and the activity of heterogeneous particles (Tiller, 1962). The amount of change in the temperature gradient and the degree of supercooling in a solidifying ingot with the distance from the chill surface is shown in Fig. 14.

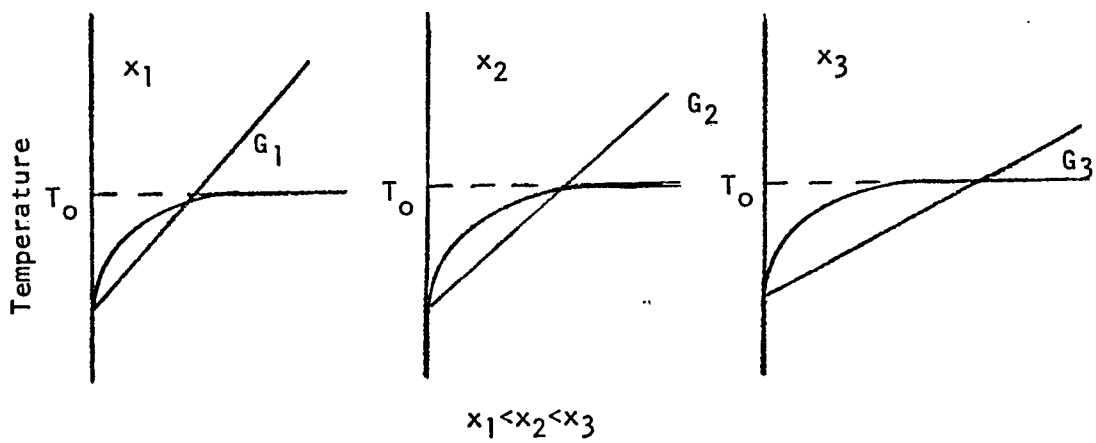

Fig. 14. Variation of G and T_l ahead of the Solid-Liquid Interface with Increasing Solidified Metal Thickness, x.

The number of new nuclei formed at the interface may be approximated by the expression

$$N \sim f(x^2) \cdot f(\text{supercooling})$$

where x is the thickness of metal solidified. As x increases, solute concentration at the dendrite tips increases and supercooling decreases.

The parameters which affect the length of the columnar zone of an alloy ingot can be summarized. The zone decreases with:

a. Decreasing superheat.

b. Increase in alloy freezing range.

c. Increasing number and catalytic activity of the nucleation centers.

d. Decreasing interface motion.

e. Increasing ingot length.

f. Liquid stirring.

A large degree of superheat establishes a steep initial thermal gradient, G. An alloy with a large freezing range tends to have a "mushy" or "pasty" type of solidification which is discussed by many authors (Cibula, 1950; Ruddle and Mincher, 1950; Engles, 1969). A great deal of research has been done on catalytic agents to acquire fine-grained equiaxed structures in alloy castings (Cibula and Ruddle, 1949). The effects of stirring and interface motion on the length of columnar crystals have been investigated and shown effective (Wojciechowski and Chalmers, 1968; Korolkov, 1963).

The columnar crystals of an alloy are a classic example of interdendritic segregation. The dendrite spines contain the least solute while the interdendritic regions are progressively richer in solute. The overall structure is typical of cored one-phase alloys. This structure is somewhat modified in two-phase alloys.

Most commercial non-ferrous alloys are two-phase. The second phase is normally dispersed sub-microscopically in a primary phase matrix. At higher solute concentrations (C_o in Fig. 15), a visually distinct two-phase structure is obtained upon solidification.

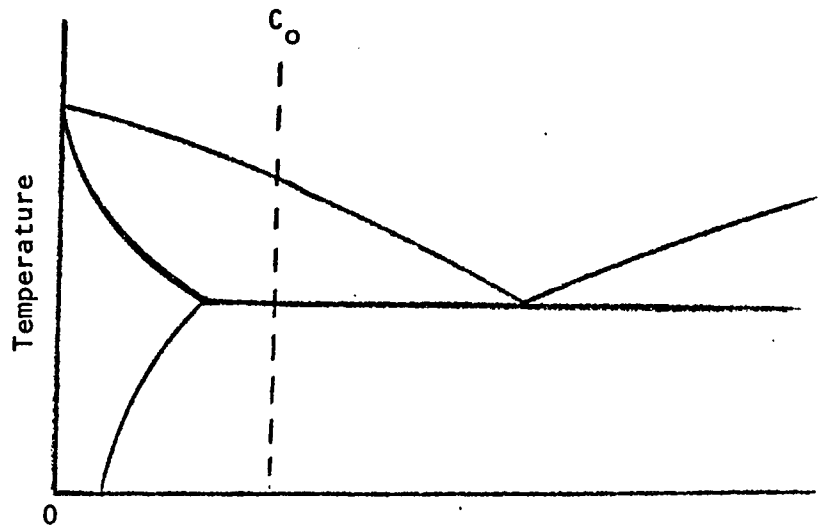

Fig. 15. A Portion of a Two-Phase Alloy Phase Diagram.

The eutectic will solidify interdendritically under conditions of unidirectional solidification. It has been shown (Cahoon and Paxton, 1969), that in a direction parallel to the heat flow, an increase in strength was observed over randomly oriented crystals. The analysis of this phenomenon was that of a fiber reinforcement mechanism of the interdendritic eutectic. The volume fraction of eutectic obtained in the solidification of an alloy of composition C_o may be calculated from:

$$f_e^o = (C_s/k_oC_o)^{(1/k_o-1)}$$

where:

f_e^o = Volume fraction of eutectic.

C_s = Solubility limit at the eutectic temperature.

k_o = Equilibrium partition coefficient.

C_o = Base composition of the alloy.

This quantity of material, when arranged in a continuous elongated structure, can be thought of as the fiber component in a composite structure which was described earlier.

The lever law calculation of the eutectic fraction applies only for equilibrium cooling. Since the solidification methods being described are far from equilibrium conditions, the non-equilibrium calculation above is more applicable.

Fiber Strengthening

The mechanics of the fiber strengthening mechanism were developed during the early investigations of composite materials. The mechanical properties of a composite can be estimated from the properties of its components (Kelly, 1966). For example, the yield strength of a fibrous material may be estimated by

$$\sigma_{ys} = (\sigma_m(1-V_f)) + (\sigma_f \cdot V_f(1+) \cdot (w1-))$$

$$+ ((V_f - V_f(1+)) \cdot (\tau 1-)/d)$$

where:

σ_{ys} = yield strength of the composite or alloy.

σ_m = yield strength of the matrix material.

σ_f = yield strength of the fibers.

V_f = total volume fraction of fibers.

$V_f(1+)$ = volume of fibers whose length is greater than a critical minimum.

$1-$ = the average length of fibers which are shorter than the critical minimum.

w = a factor less than one which depends on fiber length and matrix plasticity.

τ = shear strength at the fiber-matrix interface.

d = fiber diameter.

During the past twenty years, many researchers have been working on techniques to attain fibrous structures in eutectic alloys. Both lamellar and rod-like structures have been made with varying degrees of success (Chadwick, 1964). Many alloy eutectics, such as Al-33Cu, can be solidified into a material having a ductile matrix (primary aluminum) surrounding strong hard fibers ($CuAl_2$). Some fibers which have been grown are close to metal whiskers in strength (Salkind and Lemkey, 1967).

The fiber strengthening equation applies to both eutectic and off-eutectic compositions. The differences lie in the modes of solidification. Directional eutectics are grown slowly like platelets in pure metals where off-eutectics are subject to constitutional supercooling. Comparing solid-liquid interfaces, one is planar and the other is dendritic.

It was discovered many years ago (Roberts-Austen, 1897) that fully eutectic-like structures can be obtained in alloys which are slightly off the eutectic composition. The extent to which this could be achieved was outlined by Mollard and Flemmings (1967) who used:

a. Slow growth rates.

b. Steep thermal gradients.

c. Absence of convection.

Again, the investigators have not specified what the general macrostructure

of these composites may be. We can only assume that they are random polycrystals (in the matrix, anyway).

Feather Crystals

Most commercial aluminum casting alloys are far from the eutectic composition in their solute content. Thus the solidification of these materials follows the procedures described in the section on alloys. Laboratory research has led to many improvements in casting quality (Taylor, Walther, and Adams, 1954; Sicha and Balhm, 1948). Among these is the process for producing commercial aluminum semi-stock called direct chill continuous casting. It was discovered early in the development of this process that the cast billets produced contained an unusual crystal structure (Herenguel, 1948). Other investigators (Aust, Krill, and Morral, 1952; Schipper and Roth, 1956) classified the structure as growth twinned or "feather crystal".

The most comprehensive research on the morphology of growth twin crystals has been performed in Japan (Watanabe, Honma, and Oya, 1969; Miyazawa, Honma, and Oya, 1969). The experiments were performed with pure aluminum, Al-8 Mg, Al-5 Si, Al-Cu and Al-Cu-Si alloys. Some of their significant findings were:

a. Feather crystals were nucleated by two-dimensional sites located at lattice imperfections such as grain boundaries, stacking faults, pores, and inclusions.

b. Multiplication of twins was found to occur on the growing interface of the twin crystals and not in the columnar or equiaxed crystals.

c. The twin plates are 30 to 100 microns in thickness and grow in the direction parallel to heat removal.

d. The twin plane is {111} and the direction of preferential growth is <112>. Faceted {100} planes grow at 54.7 degrees to the twin plane.

e. A minimum amount of solute concentration was required for the observation of feather crystals. Also, at higher solute concentrations feather crystals were not observed. The range of concentration of solutes for feather crystal occurrence was: 11 to 19% Mg, 3 to 10% Sn and 0.06 to 0.17% Ti.

f. Macroscopic segregation along the length of an ingot was found to vary less for feather crystals than for columnar crystals when solidified from melts of similar composition.

In finding c, the authors failed to note that feather crystals usually display a "fan" pattern in an ingot. If growth is parallel to the direction of heat removal, then the feather crystal nucleation site must be the key location of heat removal.

Unlike columnar crystal dendrites, feather crystals have a lamellar distribution in a cast ingot. A schematic representation of this structure is shown in Fig. 16.

Other mechanisms of feather crystal nucleation were proposed prior to the work of Watanabe et al. (1969). One is the re-entrant edge mechanism (Wagner, 1960) similar to that observed in germanium crystal twins. Another speculation is a form of lateral layer growth (Cahn, Hillig, and Sears, 1964). In an experiment where decantation interfaces were examined (Morris, Carruthers, Plumtree and Winegard, 1966), another conclusion was drawn. These investigators concluded that the nucleating mechanism for feather crystals could not be readily determined. They did observe, however, that once nucleated, feathery dendrites did grow faster than columnar grains. The explanation given for this phenomenon is based on the condition that less solute is built up in front

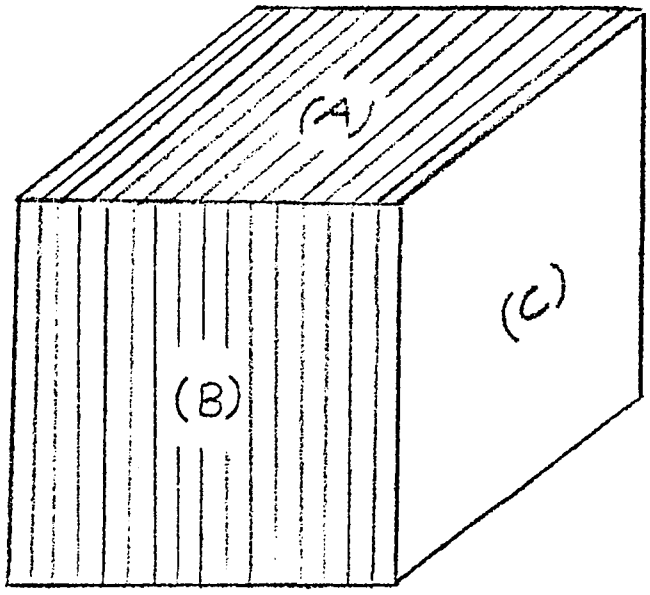

Fig. 16. Unidirectionally Solidified Cast Block Showing the Orientation of Feather Crystals.

(A): Short transverse section
(B): Long transverse section
(C): Longitudinal section

of the growing crystals. It was shown that feather crystals have a more efficient form of solute redistribution and grow at higher temperatures than the columnar dendrite tips. Therefore, feather crystals grow ahead and win out in competitive growth.

The morphology of feather crystals has been investigated in many ways. Watanabe et al. (1969) used x-ray diffraction, electron microscopy and dislocation etching (Barrett and Levenson, 1940). The etch pits observed suggested that dislocations or lattice faults were distributed symmetrically about the {111} twin plane. Morris et al.

(1966) utilized polarized light microscopy on samples which had a thin anodic film deposited on the polished surfaces. Other authors used microscopy (Walker and Benn, 1971a), electron microprobe analysis, and autoradiography (Wojciechowski and Wallis, 1969).

In the investigation by Morris et al., it was shown that both a critical growth rate and a minimum solute concentration was required to depart from columnar crystal growth (Nakao, 1957). These values were given as R_{min} = 2.4 cm/sec and the critical solute concentrations of 0.04% Ti, 2% Cu or Mg, and 8% Zn. These results contrast with the original opinions of the early investigators who believed that growth twinning increased with increasing aluminum purity.

In a recent paper (Gullman and Johansson, 1972), an analysis of feather crystal occurrence in direct chill continuous cast commercial aluminum was presented. The results of this investigation may be summarized by:

a. Two conditions are necessary to nucleate feathery crystals in cast aluminum: the presence of certain alloying elements in the melt and a cooling rate of about 1000 degrees C/sec.

b. If the cooling rate is high enough, the number of twin crystals nucleated is proportional to the area of the chill surface and the concentration of the twin-producing alloying elements.

c. Under identical solidification conditions, the following elements were found to have the same tendency to form feather crystals. The minimum concentrations required were: 0.015% Ti, 0.85% Fe, 1.10% Ni, 1.30% Mg, 2.90% Sn, 3.50% Cu, 5.55% Si and 6.45% Zn.

d. Growth twin crystals can be eliminated from continuous cast aluminum by adding an effective grain refiner or by stirring the melt.

The authors seemed convinced that since iron is the most common impurity found in commercial aluminum, it must be effective in the nucleating of feather crystals. They conducted a number of experiments with increasing iron content in pure aluminum. The results were reported as a "fundamental uncertainty" in the determination of a concentration dependence of the feathery structure.

In comparing the summary of Gullman and Johannson with the findings of Morris et al. and Watanabe et al., most of the conditions for feather crystal nucleation coincide. The only outstanding difference was the high value for the minimum concentration of magnesium required for nucleation which was reported by the Japanese investigators.

In all of the investigations cited, no evaluations of the mechanical properties of feather crystals were reported. Several properties have been reported for unidirectionally solidified superalloy turbine blades (Versnyder and Piearcey, 1966, 1967, 1969). The structures created by their technique were both columnar and single crystal. The creep properties were substantially improved and were related to the structure (Webster and Piearcey, 1966; Piearcey, Kear and Smashey, 1967).

Other investigations included the directional casting of steel (Nereo, Polich, and Flemmings, 1965) and the properties of the resulting structures (Polich and Flemmings, 1965). No substantial increase in strength was observed and in no case were feather crystals reported. After an extensive literature review, the only reported occurrence of feather crystals was in aluminum and aluminum base alloys. Also, the review showed a complete absence of mechanical property data on feather

crystals. One brief quotation on the dimensional stability of directionally cast aluminum was noted (Walker and Benn, 1971b).

OBJECTIVES

The objectives of this experiment were to evaluate some of the mechanical properties of several unidirectionally solidified aluminum alloys. The results of these evaluations were to be compared to the properties obtained by conventional casting techniques. The behavior of samples which contained columnar grains and feather crystals were to be evaluated on a comparative basis with samples having a random structure.

Another objective was to investigate the parameters involved in the unidirectional solidification of aluminum alloys to obtain feather crystals. Finally, the dimensional stability of cast mirror blanks was to be determined by thermal cycling. Again, the evaluation was to be on a comparative basis for the three types of structures.

EXPERIMENTAL

Unidirectional Solidification Experiments

Unidirectional solidification experiments were performed to evaluate the parameters involved in the formation of feather crystals. Ingots of pure aluminum (99.995%), Tenzalloy, K01, and several aluminum-copper alloys were solidified under controlled conditions. The Al-Cu alloys were made up from the pure aluminum and 99.995% pure copper. Nine alloys including the Al-33 Cu eutectic composition were made up for evaluation.

The apparatus used in the experiment is shown schematically in Fig. 17. The experiment was designed to hold a melt of alloy in a superheated state until a chill was applied to one surface. Solidification was initiated by a 10 liter/minute flow of water against a thin stainless steel plate which served as the base of the melt container. A variable gradient Marshall furnace provided a controlled melt zone three inches in diameter by 24 inches long. The furnace temperature was regulated with a Barber Colman relay-type controller.

The instrumentation for the experiments consisted of six chromel-alumel thermocouples connected to a 12-point Honeywell recorder. The thermocouples were located in the wall of the ingot crucible at various heights above the base plate and one was at the base plate. The height of the thermocouples with respect to the base plate were: 0, 0.5, 1.0, 2.0, 3.0 and 5.0 inches.

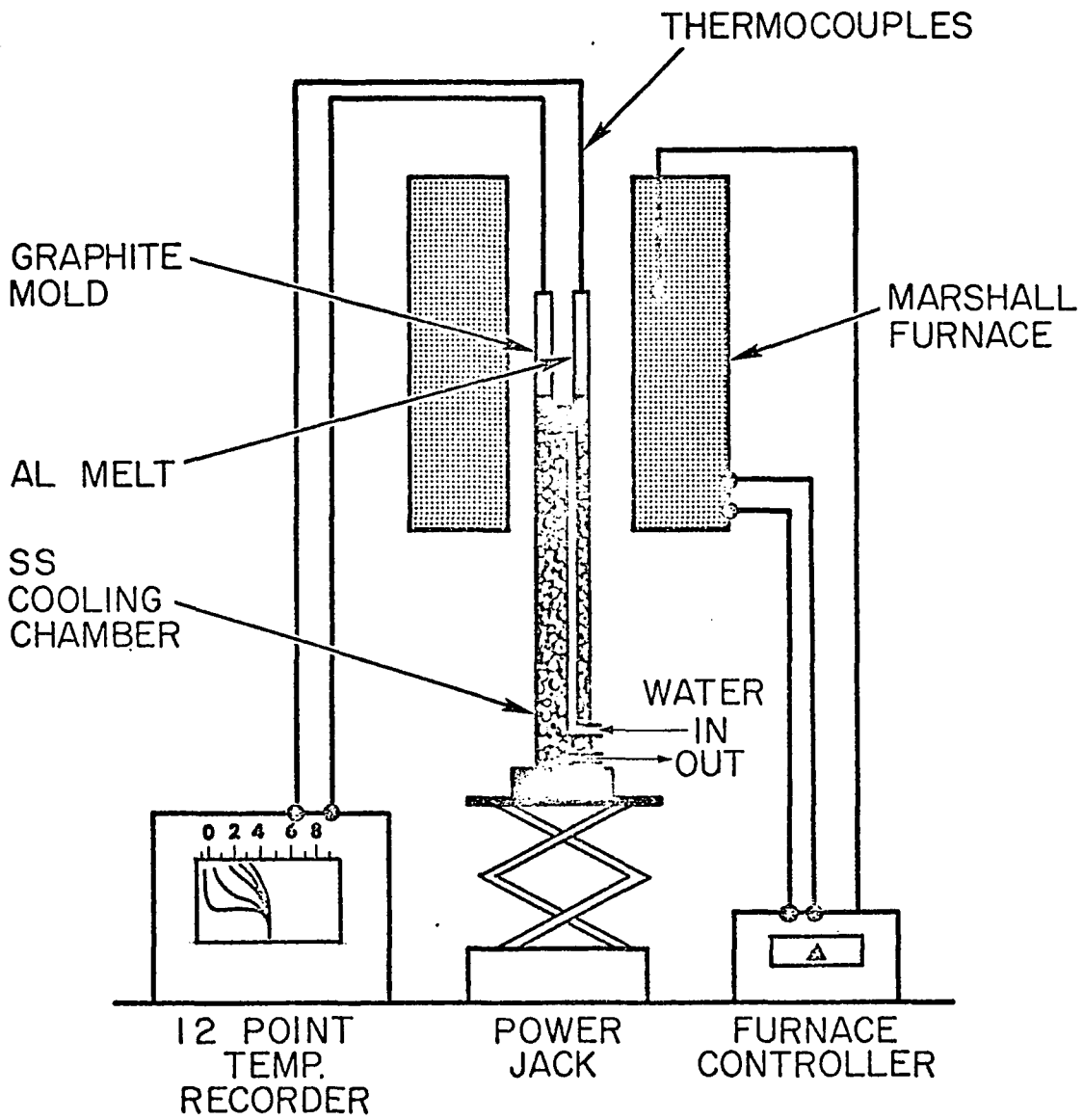

Fig. 17. Experimental Apparatus used for the Unidirectional Solidification Experiments.

The alloys were pre-melted in a resistance furnace, poured into the experimental mold and allowed to solidify. The mold and the solidified ingot were moved into the melting zone of the Marshall furnace by the power jack. After installation of the thermocouples, the furnace was turned on and the controller set at 1400°F. A melt thermal soaking period of one hour was allowed before the chill water was applied. Solidification was promoted by applying the chill water to the base plate and withdrawing the mold from the furnace at approximately 0.5 inches/minute. Complete solidification of a seven-inch ingot took about nine minutes. A typical temperature profile of an experiment following the water chill is shown in Fig. 18.

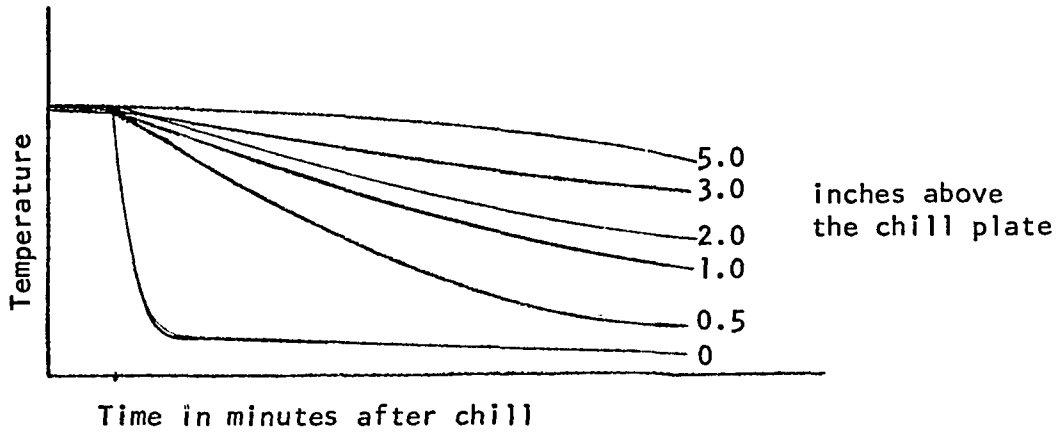

Fig. 18. Temperature Response to Chilling at Various Distances from the Chill Surface of a Unidirectionally-Solidified Aluminum Alloy Ingot.

Results of the Unidirectional Solidification Experiments

The unidirectional solidification experiments were evaluated metallographically. The ingots of Al-Cu and the commercial alloys were removed from the mold and sectioned longitudinally by milling. They were then polished and etched to reveal the grain structure. The ingot structures obtained are shown in Figs. 19 and 20.

No feather crystals were found in the ingot of pure aluminum. This observation agrees with the findings of many of the investigators. The structure obtained was totally columnar. Feather crystals were observed in the K01 ingot and were present over the entire length of the 356 ingot. The Tenzalloy sample showed feather crystals blended with columnar grains.

In the Al-Cu alloy samples, feather crystals were observed in the 3% and 6% Cu ingots but were absent in the Al-10Cu ingot. This lower limit was in agreement with the findings of Nakao but below the 3.5% minimum concentration prescribed for feather crystal nucleation by Gullman and Johannson. Under the conditions of the experiment, it appears that the feather crystals are nucleated in the concentration range of 3% to 10% copper in aluminum. Finally, the unidirectionally solidified structure of the Al-33%Cu eutectic could not be described by any of the structural types thus far discussed.

The parameters G and R were calculated from the temperature-time data. G varied from 8000°F/min at the chill surface to 40°F/min at five inches from the chill surface. The variation of R at the same locations was from 1.25 to 0.862 in/min.

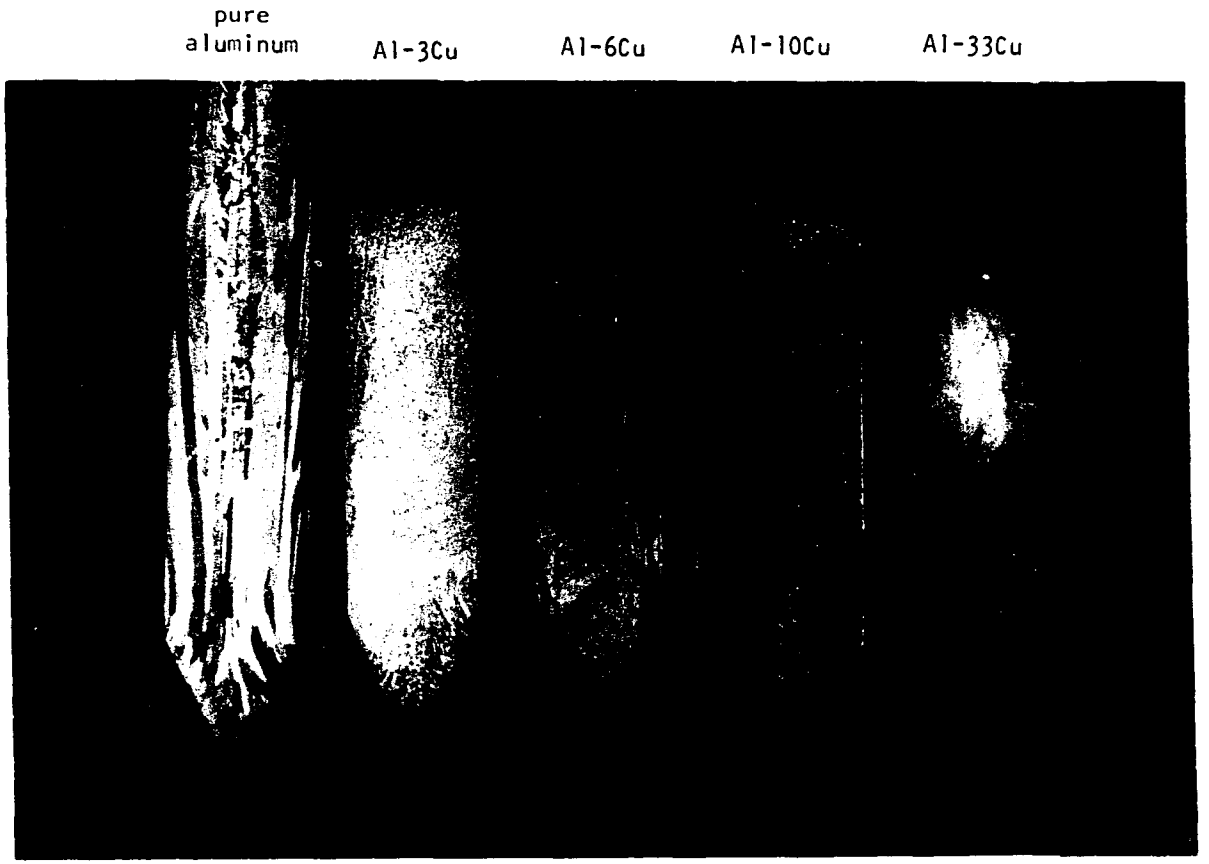

Fig. 19 The Structures of Unidirectionally Solidified Pure Alumimum and Aluminum-Copper Alloys.

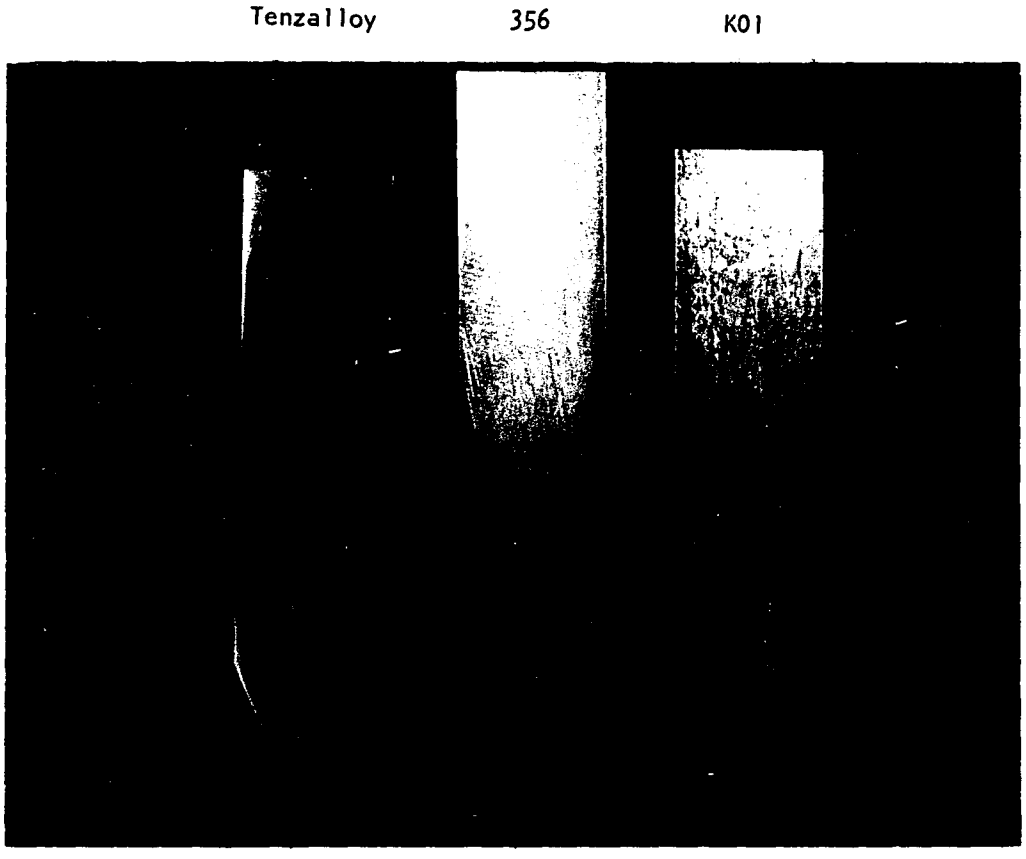

Fig. 20. The Structures of Unidirectionally Solidified Commercial Aluminum Alloys.

Conventional Casting Experiments

In this part of the investigation, samples of unidirectionally solidified alloys were made and mechanically tested. The casting methods used were practically adaptable to current aluminum foundry practice. The casting preparation for obtaining these samples goes under the general category of investment casting.

A smooth tapered pattern (see Fig. 21) which could be easily removed and re-used, was the simplest design which could supply the required test samples. The pattern was placed with its small surface down on a board and centered in a four-inch diameter steel pipe. The investment (Kerr K-90), which is a blend of gypsum and silica, was slurried and poured into the pipe. After hydration, the pattern was removed and the mold was dried for six hours at 200°F. The invested mold had a smooth cavity as shown in Fig. 22. After drying, the mold was placed in an electric resistance furnace and heated at 1290°F overnight.

Casting was performed by melting pieces of virgin alloy pigs in the College of Mines Inducto 15 high frequency induction melting apparatus shown in Fig. 23. The molten alloys were superheated to 1400°F as indicated by a chromel-alumel immersion thermocouple. A preheated alumina crucible was used to transfer the molten metal from the induction melter to the mold. In rapid succession, the mold was withdrawn from the furnace, placed on a water cooled copper chill plate (Fig. 24) and filled with molten metal.

Immediately after filling the mold with the alloy melt, a topping of "hot top" exothermic powder was placed on the exposed molten

Fig. 21. Pattern for Conventional Casting.

Fig. 22. Invested Casting Mold.

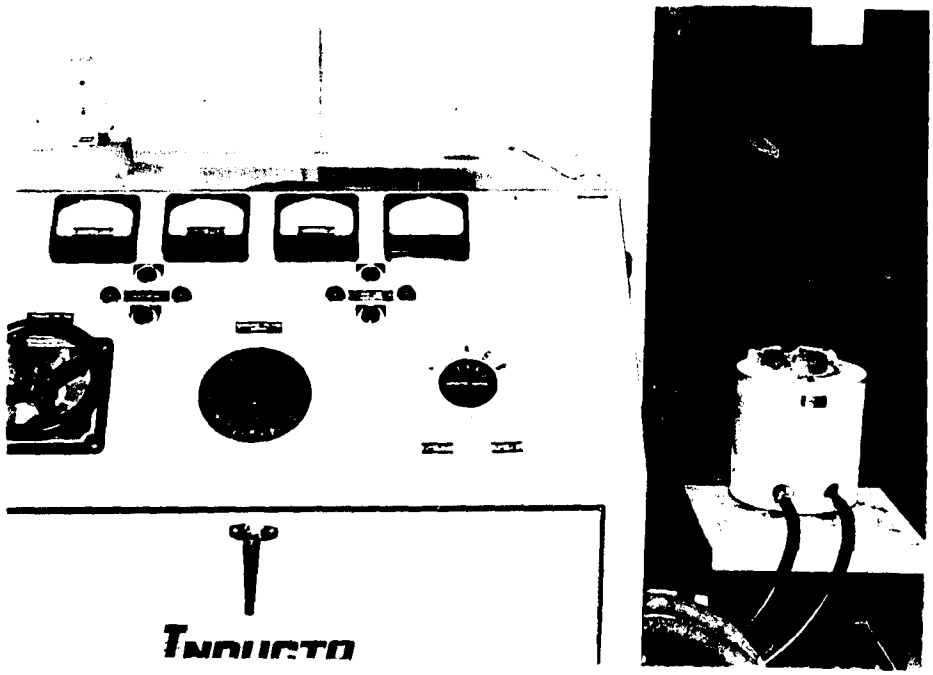

Fig. 23. The College of Mines Induction Melting Facility.

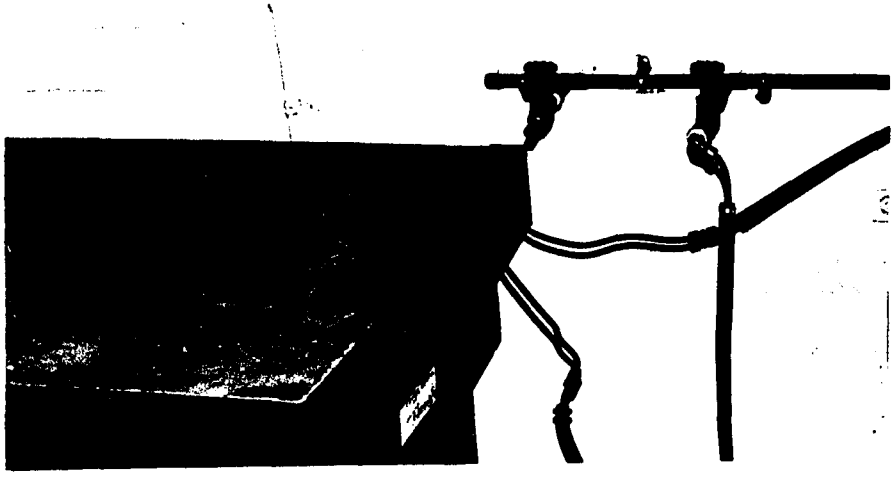

Fig. 24. Water-Cooled Copper Chill Block.

metal surface. This was to prevent solidification from originating at the top of the casting.

After cooling down, the casting was broken out of the mold and both the flash (metal exuded on the chill plate) and the pouring top were removed. It was then sectioned longitudinally and milled into two plates of 3 x 5 x 0.125 inches each. The cast structures were revealed by macroscopic etching. The macrostructure of an unmachined 356 alloy casting is shown in Fig. 25. After sectioning, milling and re-etching, the cast structure appeared as shown in Fig. 26. Fig. 27 shows three machined and etched Tenzalloy castings.

Four tensile test bars were cut from each 3 x 5 inch plate. One of these was a 3 x 3/4 inch bar cut transverse across the top section of the plate. This part of the casting had an equiaxed random grain structure as revealed by the macroetching. The other three bars were cut longitudinally from the remaining directionally structured plate material. The bars were trimmed to dimensions acceptable for tensile specimen preparation. ASTM standard sheet metal tensile specimens with a one-inch gage length were made on a Tensilcut machine. Finished and etched Tenzalloy test bars are shown in Fig. 28.

Each tensile test bar was identified by number and classified as to the structure type predominant in the gage length. Thickness and width measurements were made along the gage length of each test bar with a micrometer. These data were recorded.

The etched surfaces of the tensile bars of directionally cast alloys showed an elongated grains. Columnar crystals were revealed as elongated grains of varying widths. Feather crystals appeared as

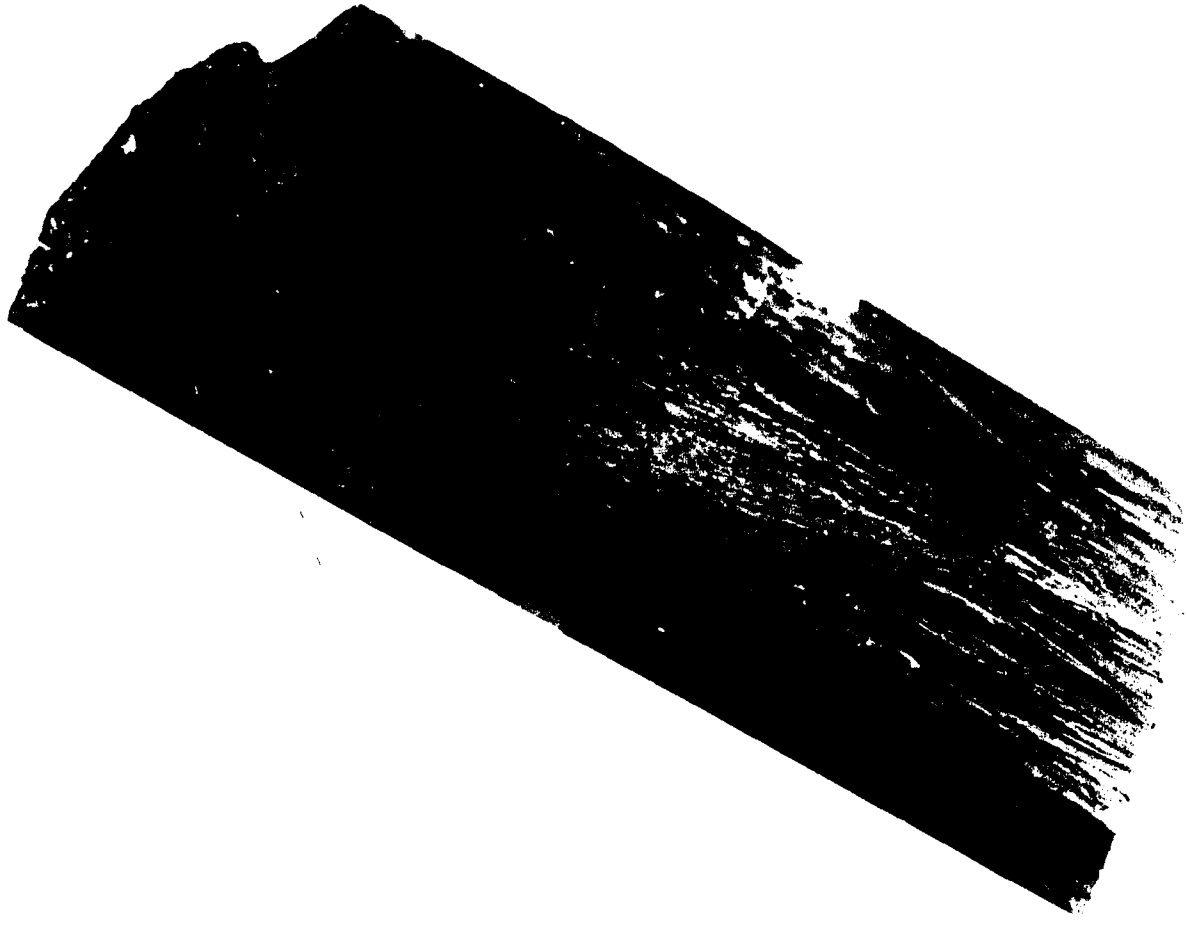

Fig. 25. Directionally Solidified Ingot of 356 (Tuckers Etch). The Edge Shows that Feather Crystals Grow Faster than Columnar Crystals.

Fig. 26. Casting of 356 Alloy after Milling Flat and Macroetching (Tuckers Etch).

Fig. 27. Three Tenzalloy Directional Castings which were Etched after Milling (Hot NaOH - Dilute HNO_3).

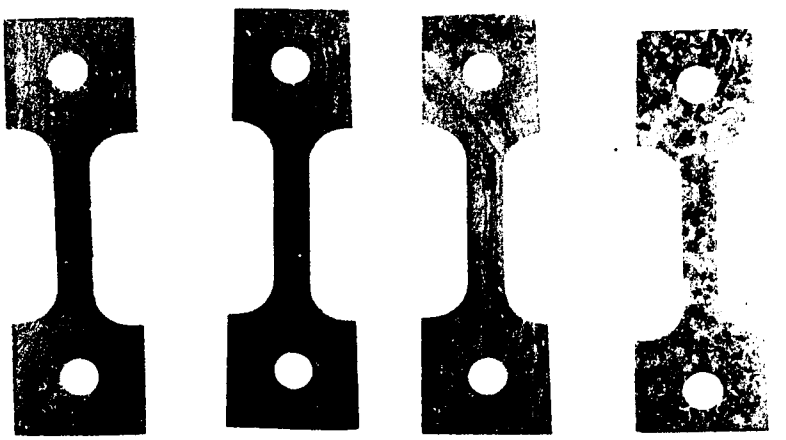

Fig. 28. Typical Tenzalloy Tensile Test Bars Before Tensile Testing. From the Left: Fine Feather Crystal, Coarse Feather Crystal, Columnar and Random Structures.

edges of platelets which intersect the surface. The lamellar edges are traces of the {111} slip planes of feather crystals. If the tensile axis is defined as a straight line connecting the pinhole centers of a tensile bar, then an angle can be measured between this line and the linear grain structure. This angle (hereafter referred to as the "structure angle"), was measured and recorded for each tensile bar with directional grains.

Pin-type tensile bars were used as opposed to the flat-grip type specimens. This was to avoid the possibility of inducing a bending stress in the sample during testing. Also, with the pin-type grip, the possibility of slippage in the grips during testing was eliminated.

Tensile testing was done on the Department of Metallurgical Engineering Instron tensile testing machine. The instrumentation was calibrated to record tensile loads up to 2000 pounds. The strain rates applied to the samples were 0.2 and 0.05 in/min. The data recorded in the testing were the ultimate tensile load in pounds and the cross-head travel in inches. The latter quantity was labeled as the elongation of the one-inch gage length. The values obtained for load were calculated with the dimensions of each test bar to evaluate the ultimate tensile strengths. The apparent yield strength was estimated from the elastic portion (up to initial deviation from) of the load-elongation curves.

The preferred orientation of the structures being tested (random, columnar, and feather crystals) was examined by x-ray diffraction analysis. Pinhole diffraction patterns of Tenzalloy test bars with the

structures shown in Fig. 28 were taken on the Metallurgical Engineering Department x-ray diffraction apparatus shown in Fig. 29. The Laue back reflection method was used with unfiltered Kα radiation.

During the testing, a wide variation of fracture surfaces were observed. This suggested a necessity for a microscopic fractography investigation. Tensile fracture surfaces of Tenzalloy were examined on a Cambridge "Stereoscan" Scanning Electron Microscope (courtesy of the Minneapolis Honeywell Co., Phoenix).

Finally, a series of tests were performed on unidirectionally solidified samples of A356 to examine the effects of heat treatment on the strength properties. Castings and tensile test bars were obtained in the manner previously described. The samples were classified as to structure and divided into four groups of nine samples each. The first was tested as-cast. The second group was solution treated at 1000°F for 10 hours and water quenched. The third and fourth groups were solution treated as group two but subsequently aged for six and 10 hours, respectively, at 310°F. The temper designation for group two was T4 and for groups three and four, T6, as outlined in the ASM Handbook, Vol. 2 (1964).

Results of the Casting Experiments

The nominal properties of cast and wrought aluminum alloys with various temper designations are shown in Table 1. The results of the tensile tests on the 356, Tenzalloy and A356 alloys are presented in Tables 2, 3, 4 and 5, respectively. Table 5 contains test values for heat treated A356. The results of the tensile tests are also presented

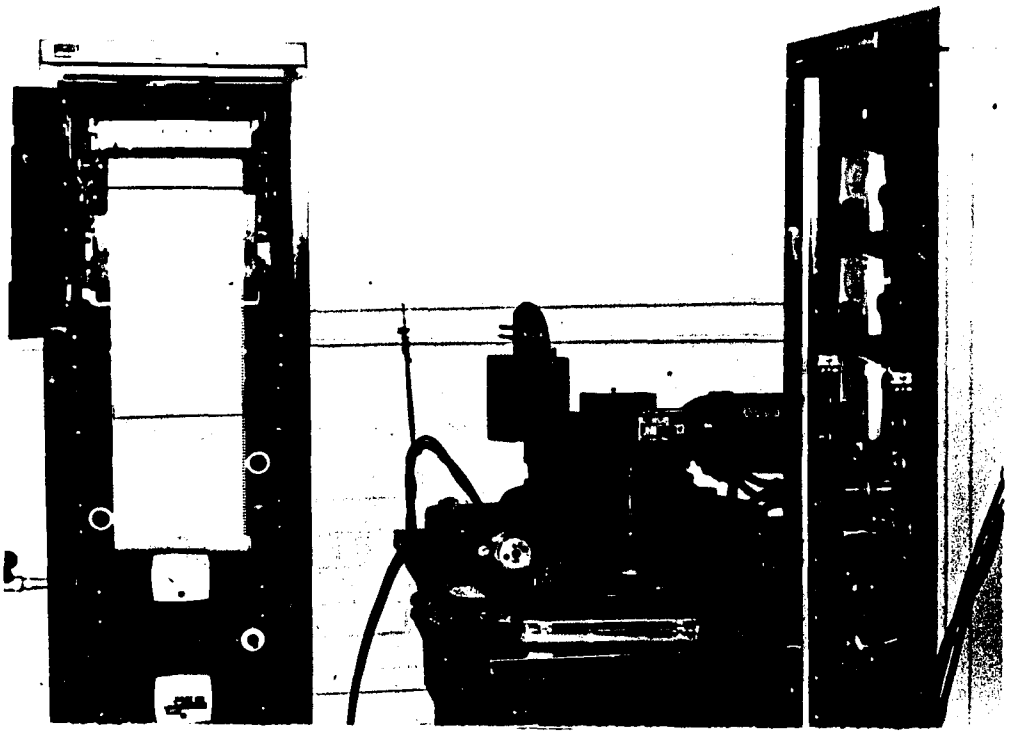

Fig. 29. The Metallurgical Engineering Department X-ray Diffraction Facility.

TABLE 1

Typical Properties of Cast and Wrought Aluminum Alloys

Alloy and Temper	Ultimate Tensile Strength (psi)	Yield Strength (psi)	Elongation per cent
	Cast Alloys		
195-T4	32,000	16,000	8.5
195-T6	36,000	24,000	5
356-T6	38,000	27,000	5
A356-T61	41,000	30,000	10
K01-T43	56,000	37,300	16
Tenzalloy-F	35,000	25,000	5
	Wrought Alloys		
1100-0	16,000	15,000	40
2024-0	27,000	11,000	22
2024-T6	69,000	57,000	10
6061-0	18,000	8,000	30
6061-T6	45,000	40,000	17
7075-0	33,000	15,000	16
7075-T6	83,000	73,000	13

Data from Alcoa Aluminum Handbook, 1962

TABLE 2

The Properties of Unidirectionally Solidified 356 Alloy

Sample	Structure	Ultimate Load (lbs)	Ultimate Tensile Strength (psi)	Elongation per cent
1	Random	660	19,700	3
2	Random	560	18,920	4
3	Random	625	19,750	4
4	Random	505	19,050	4
5	Random	580	19,200	3
6	Random	480	18,700	3
7	Random	605	21,200	6
8	Columnar-90°	695	23,400	12
9	Columnar-90°	785	24,800	8
10	Columnar-90°	682	21,650	11
11	Feather-70°	705	23,620	8
12	Feather-90°	530	22,650	7
13	Feather-65°	610	20,900	5
14	Feather-80°	580	21,950	8
15	Columnar-80°	760	22,500	4
16	Feather-75°	590	20,350	4
17	Feather-80°	570	22,950	7
18	Columnar-90°	738	21,100	11
19	Columnar-0°	690	23,550	9
20	Feather-20°	880	25,300	10
21	1/2 F + C-45°	800	26,550	8
22	Feather-35°	865	27,550	6
23	Columnar-0°	745	24,750	--
24	Columnar-0°	695	23,550	10
25	Feather-0°	765	25,550	8
26	Columnar-0°	730	22,000	7
27	Feather-40°	845	27,200	12

TABLE 3

The Properties of Unidirectionally Solidified Tenzalloy

Sample	Structure	Ultimate Tensile Strength (psi)	Yield Strength (psi)	Elongation per cent
1	Random	29,670	17,350	7
2	Random	29,400	--	8
3	Random	28,350	15,350	6.4
4	Random	30,800	20,000	8
5	Random	29,350	17,880	6.5
6	Random	29,700	17,850	8
7	Columnar-0°	37,700	20,500	26
8	Columnar-0°	37,780	18,650	24.5
9	Columnar-0°	36,900	20,400	22.5
10	1/2 F + C-17°	37,600	17,600	23.5
11	Columnar-0°	37,300	17,850	20
12	1/2 F + C-50°	36,600	17,350	28
13	1/2 F + C-16°	32,050	17,620	10
14	Feather-17°	39,900	21,400	21.5
15	Columnar-0°	37,250	19,150	17
16	Feather-7°	38,500	19,850	22.5
17	Feather-6°	42,200	21,150	16
18	Feather-35°	38,900	18,920	19
19	1/2 F + C-39°	37,850	21,300	15
20	1/2 F + C-30°	38,460	19,660	26
21	Feather-25°	40,700	20,100	22
22	Feather-15°	39,200	19,850	20
23	Feather-20°	38,250	19,260	24
24	Feather-24°	35,500	18,600	25

TABLE 4

The Properties of Unidirectionally Solidified A356 Alloy

Sample	Structure	Ultimate Tensile Strength (psi)	Yield Strength (psi)	Elongation per cent
1	Random	19,100	13,250	7
2	Random	20,800	11,300	11.5
3	Random	19,450	12,200	6
4	Columnar-0°	22,450	13,280	15
5	Columnar-0°	24,550	13,680	20
6	Columnar-0°	23,650	12,800	21
7	Feather-0°	24,400	14,280	11.5
8	Feather-0°	23,300	13.800	16
9	Feather-0°	23,550	14,050	13.5

TABLE 5

The Properties of Unidirectionally Solidified and Heat Treated A356 Alloy

Sample	Structure and Temper	Ultimate Tensile Strength (psi)	Yield Strength (psi)	Elongation per cent
1	Random-T4	29,650	15,300	21.5
2	Random-T4	29,700	14,050	22
3	Columnar-T4	30,500	15,000	30.5
4	Columnar-T4	32,200	14,150	36
5	Columnar-T4	30,900	14,000	40
6	Feather-T4	30,400	14,320	43
7	Feather-T4	29,800	13,900	38.5
8	Feather-T4	28,800	14,650	40
9	Random-T6	27,060	14,810	16
10	Random-T6	25,500	14,320	16
11	Random-T6	27,900	14,320	18
12	Columnar-T6	31,500	15,250	24
13	Columnar-T6	31,650	15,550	32
14	Columnar-T6	31,650	13,650	50
15	Columnar-T6	30,650	14,800	38
16	Feather-T6	32,900	15,950	36
17	Feather-T6	31,000	13,900	42
18	Feather-T6	31,400	14,820	35.5
19	Feather-T6	30,700	13,800	37
20	Columnar-T6-R	37,400	19,840	40
21	Columnar-T6-R	37,800	20,200	40
22	Columnar-T6-R	37,600	20,100	36
23	Feather-T6-R	37,100	19,200	38
24	Feather-T6-R	38,100	19,700	28
25	Feather-T6-R	32,900	17,450	44

T6-R = Re-heat treatment of T6 specimens.

graphically in Figs. 30 to 41. The values are presented with relation to alloy, temper, and the angle between the tensile axis and the traces of the directional structures which appeared on the bar surface.

The average values of the ultimate tensile strength for the three alloys tested are shown in Fig. 30. Each alloy bar graph is composed of values for the three structural types identified in this experiment. For all of the alloys, samples which had columnar and feather crystals were stronger than samples which had a random grain structure. In 356 and Tenzalloy, test bars containing feather crystals were stronger than those with columnar crystals, while in A356 the opposite was true. This may be associated with the impurity differences between 356 and A356 which will be discussed later.

The yield strengths of the Tenzalloy and A356 samples tested are presented in Fig. 31. It appeared that samples with feather crystals were again stronger than those with columnar grains for both alloys. The per cent elongation observed in the tensile testing is shown in Fig. 32. In general, samples with both columnar and feather crystals showed surprisingly high elongations. The values approach and even exceed those observed for some wrought aluminum alloys. This observation will be examined more closely in the Discussion section which follows.

The effect of thermal treatment on unidirectionally solidified alloys was evaluated and the results are tabulated in Table 5. The graphical representation of these values shows the changes in properties of the three structural types of A356 tested both before and after thermal treatment.

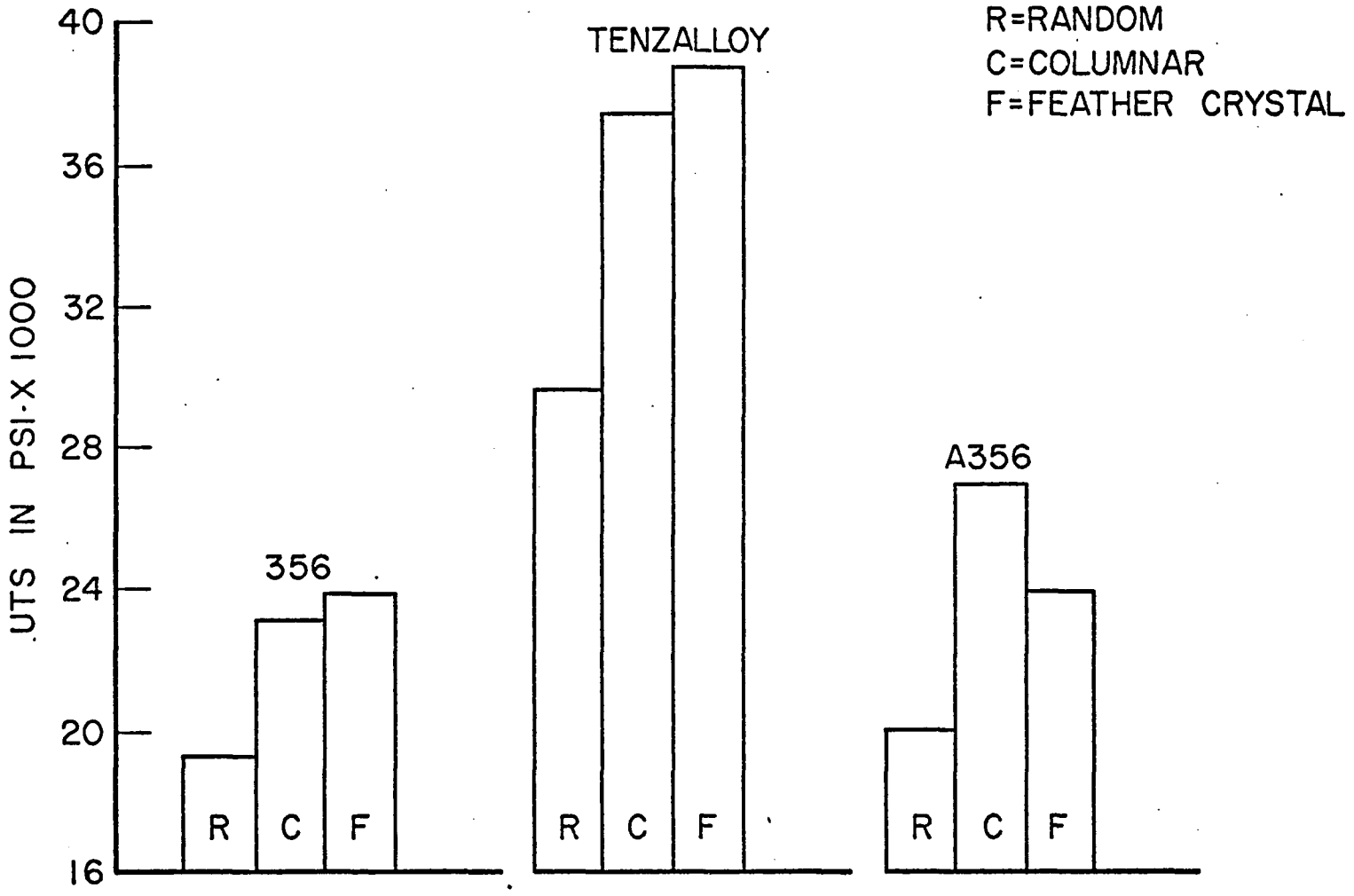

Fig. 30. The Average Values of the Ultimate Tensile Strength of the Three Alloys Tested.

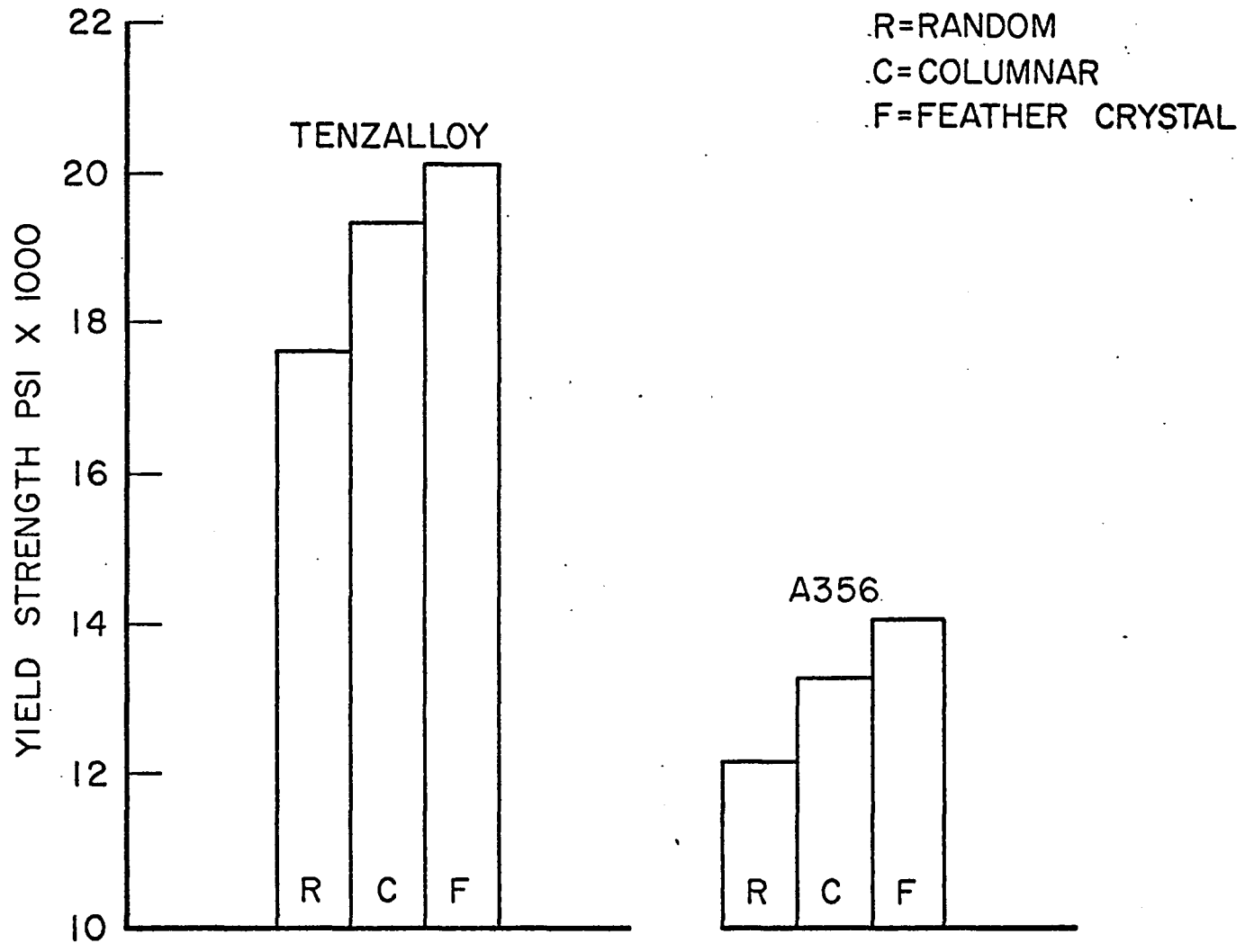

Fig. 31. The Average Values of the Yield Strength of Tenzalloy and A356.

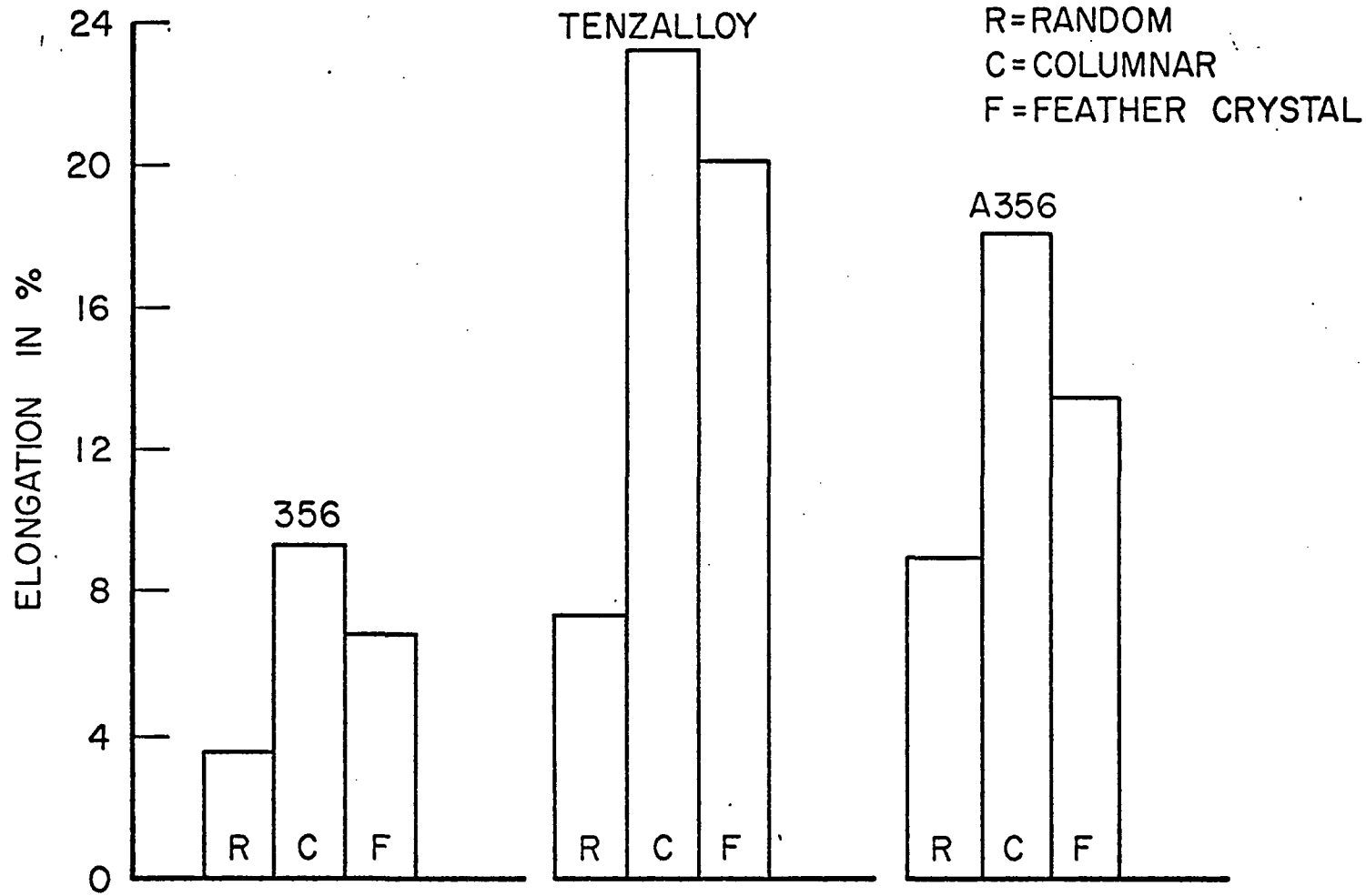

Fig. 32. The Average Values of Elongation of the Three Alloys Tested.

The ultimate tensile strengths of the three crystal structures in the as-cast, T4, and T6 conditions are shown in Fig. 33. The T4 treatment (solution treat at 1000°F for 10 hours, water quench) raised the strength of the random structure considerably more than the columnar or feather crystal structures. In the T6 condition, random structure strength decreased indicating that overaging probably occurred. The same general statements may be made for the yield strengths shown in Fig. 34.

In Fig. 35, the elongations observed in the tensile testing of the A356 samples is presented. Again, unusually high values were observed for the directionally structured samples. It appéars that the kinetics of precipitation hardening, which are optimum for randomly structured cast alloys, do not apply to castings with highly directional structures.

Due to the low nature of the T6 results, several samples were taken through the entire heat treat cycle a second time. These samples were listed in Table 5 as T6-R. The results of testing these samples are presented in Fig. 36. Unfortunately, no random structured samples were available for this test. Both the ultimate tensile and yield strengths of the columnar and feather crystal samples increased as compared to the T6 results. The slight decrease in the elongations observed further indicate that this heat treatment was more effective than the previous T6 treatment.

In Figs. 37 through 41, the values of the strength and elongation properties for the A356 samples which had directional structures are plotted against the previously discussed angle. This "structure

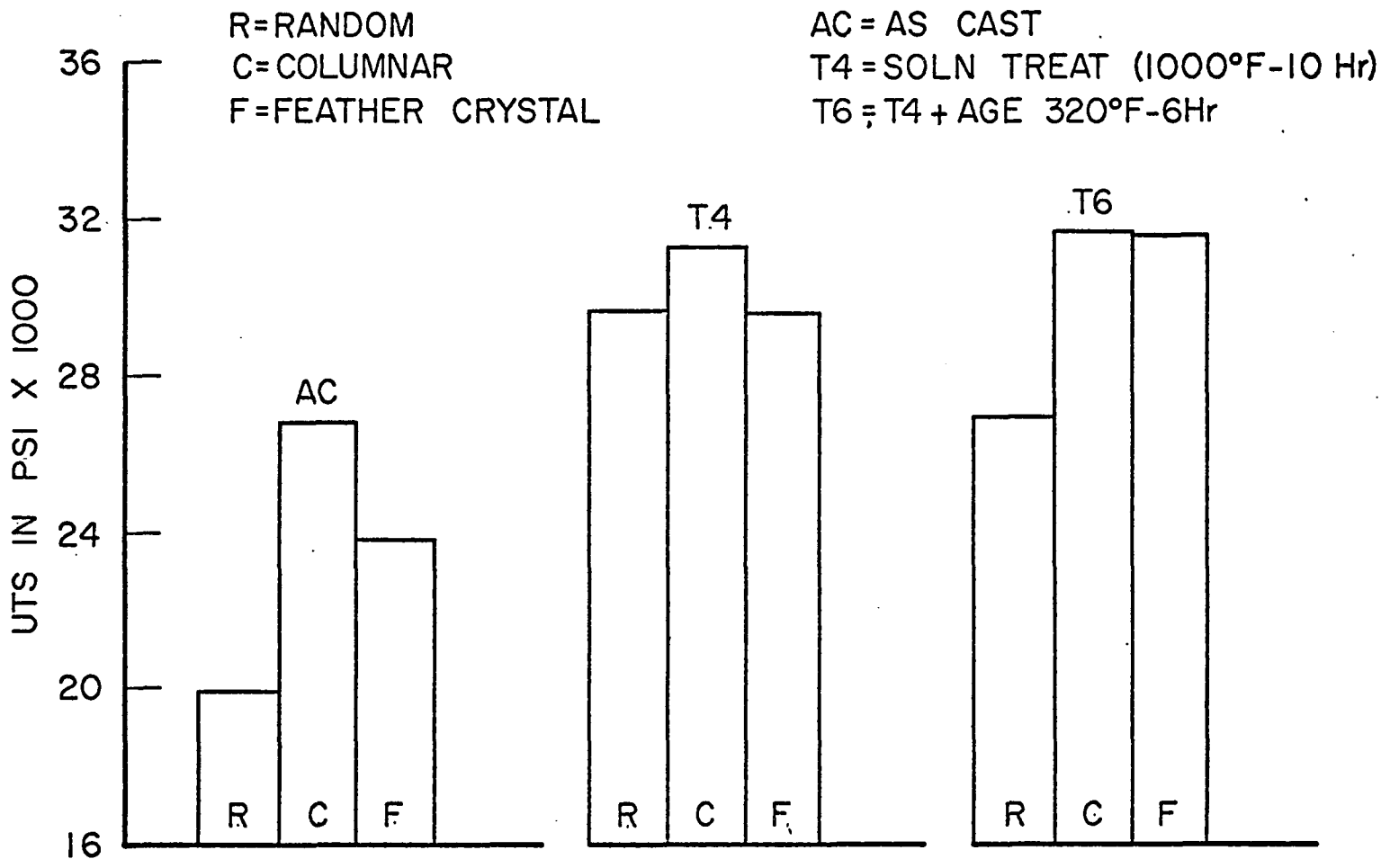

Fig. 33. The Average Values of the Ultimate Tensile Strength of A356 both Before and After Heat Treatment.

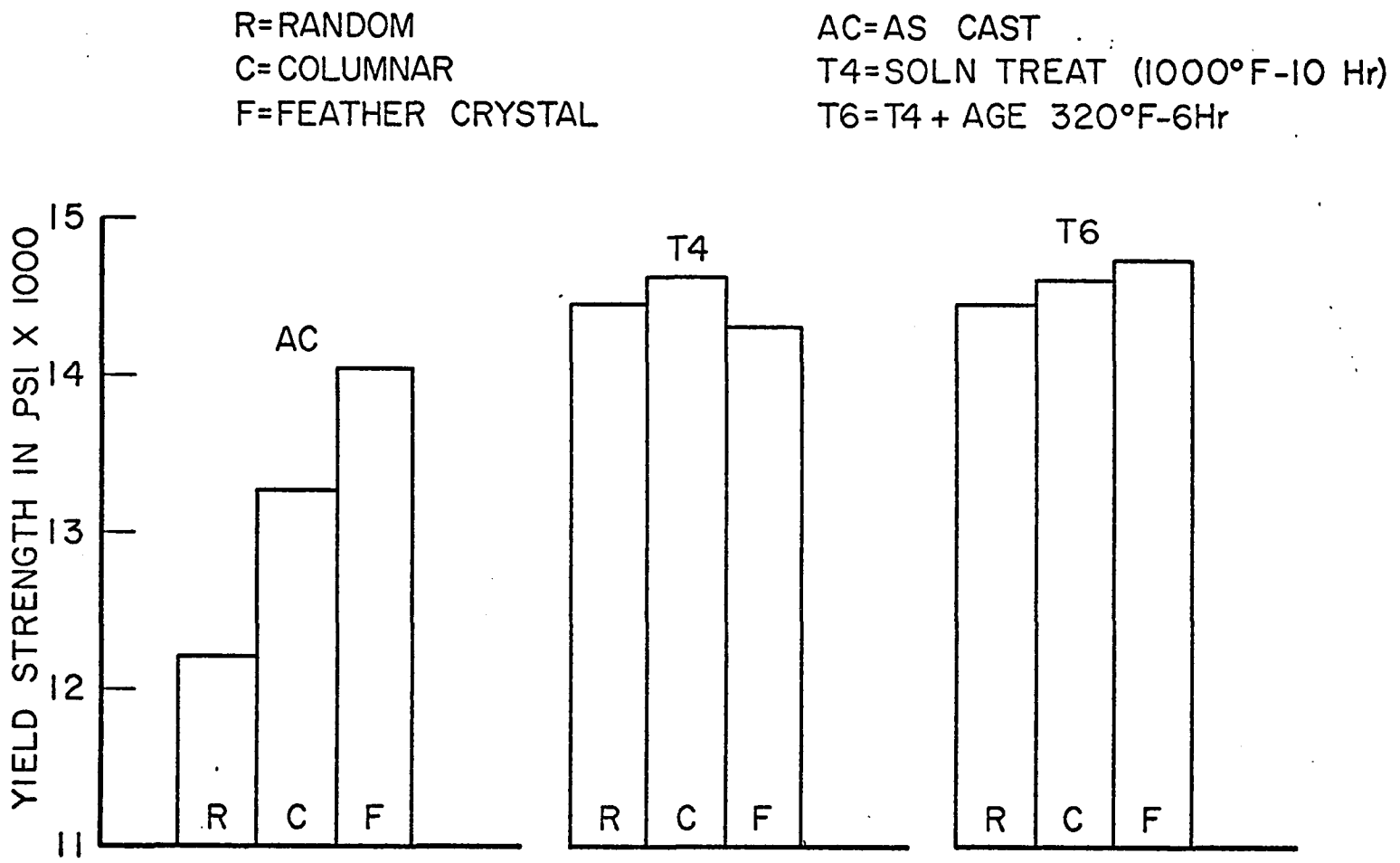

Fig. 34. The Average Values of the Yield Strength of A356 both Before and After Heat Treatment.

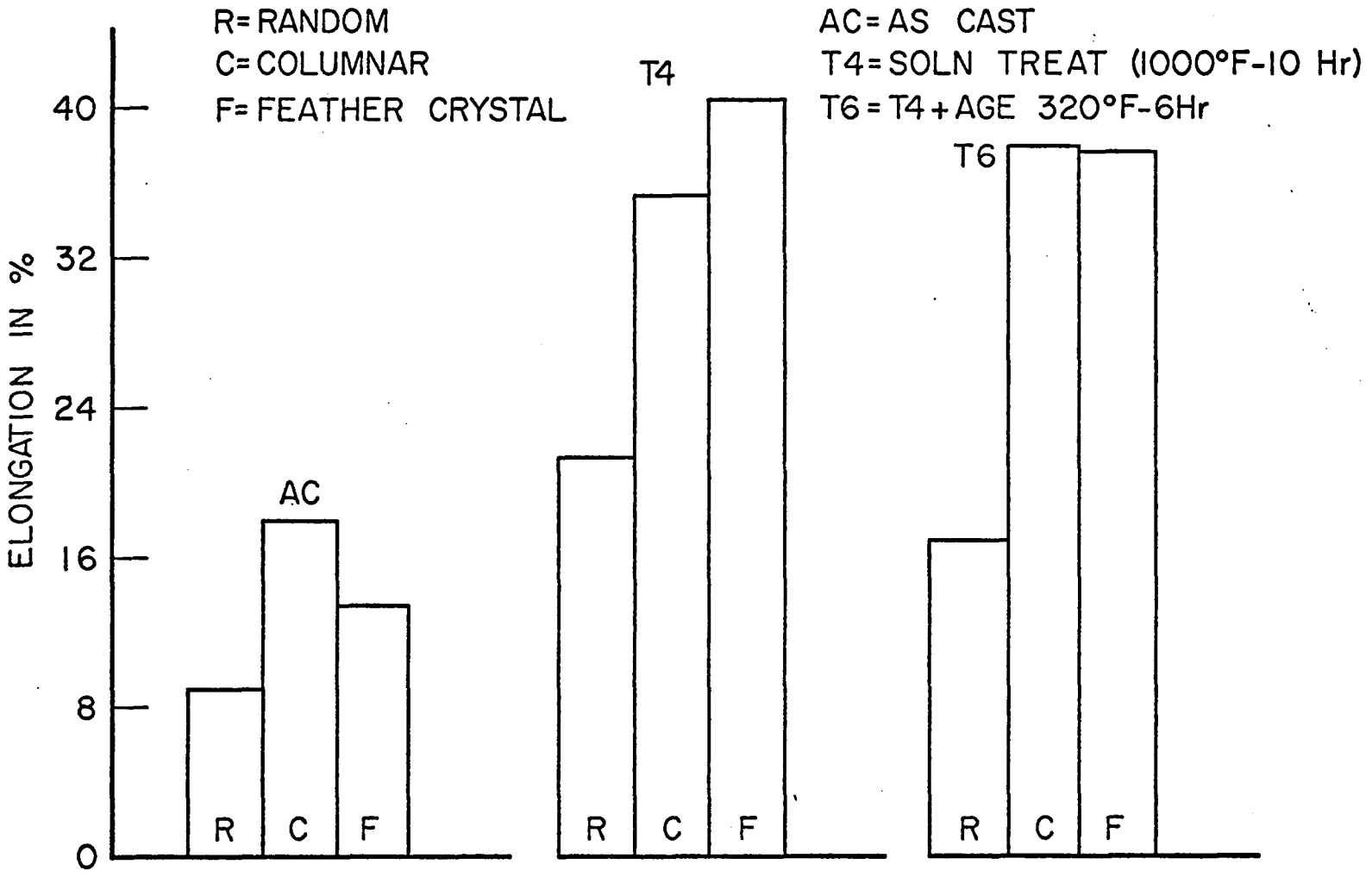

Fig. 35. The Average Values of Elongation of A356 both Before and After Heat Treatment.

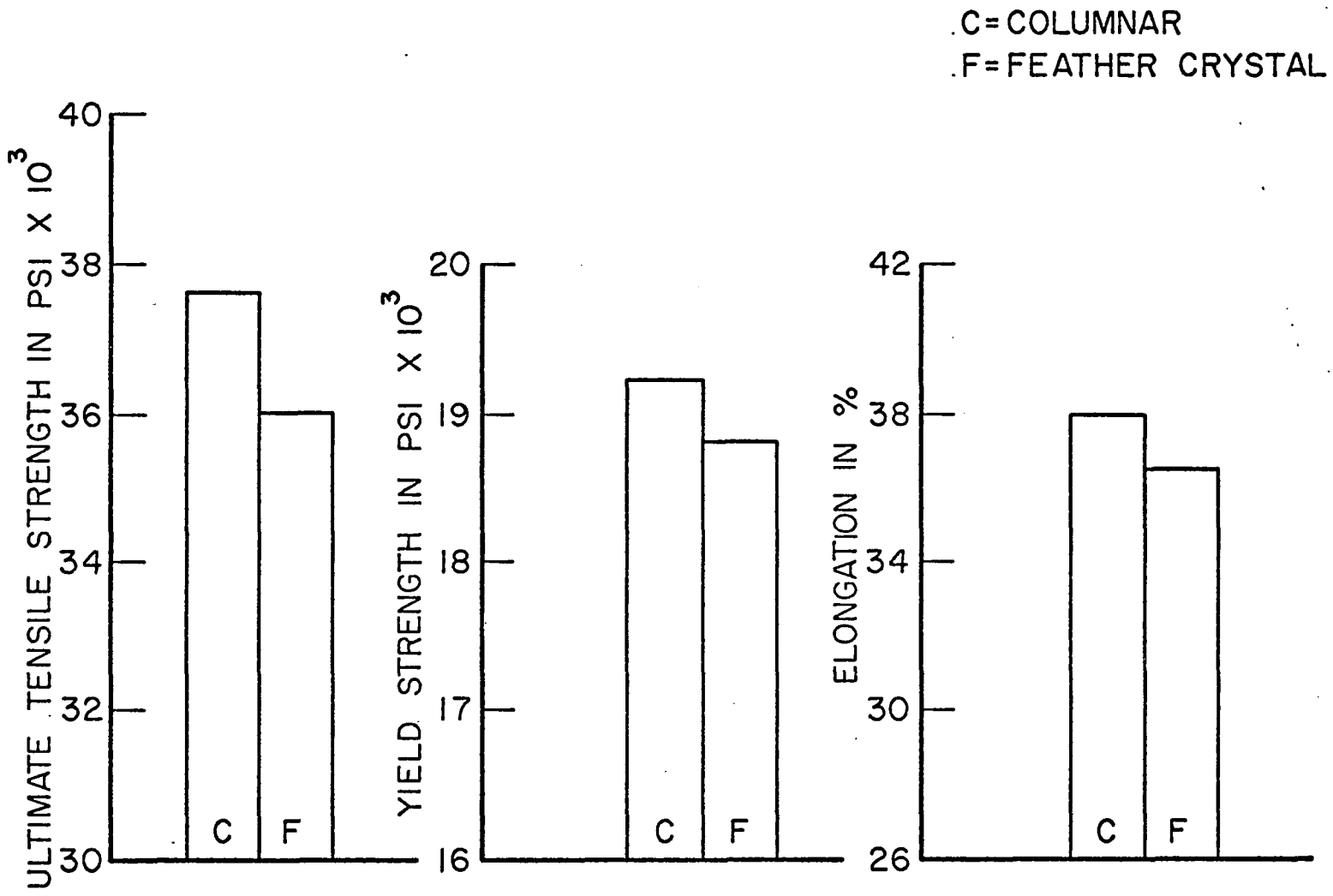

Fig. 36. The Average Values of the Ultimate Tensile Strength, Yield Strength and Elongation of A356 Test Bars which were Re-Heat Treated to the T6 Condition.

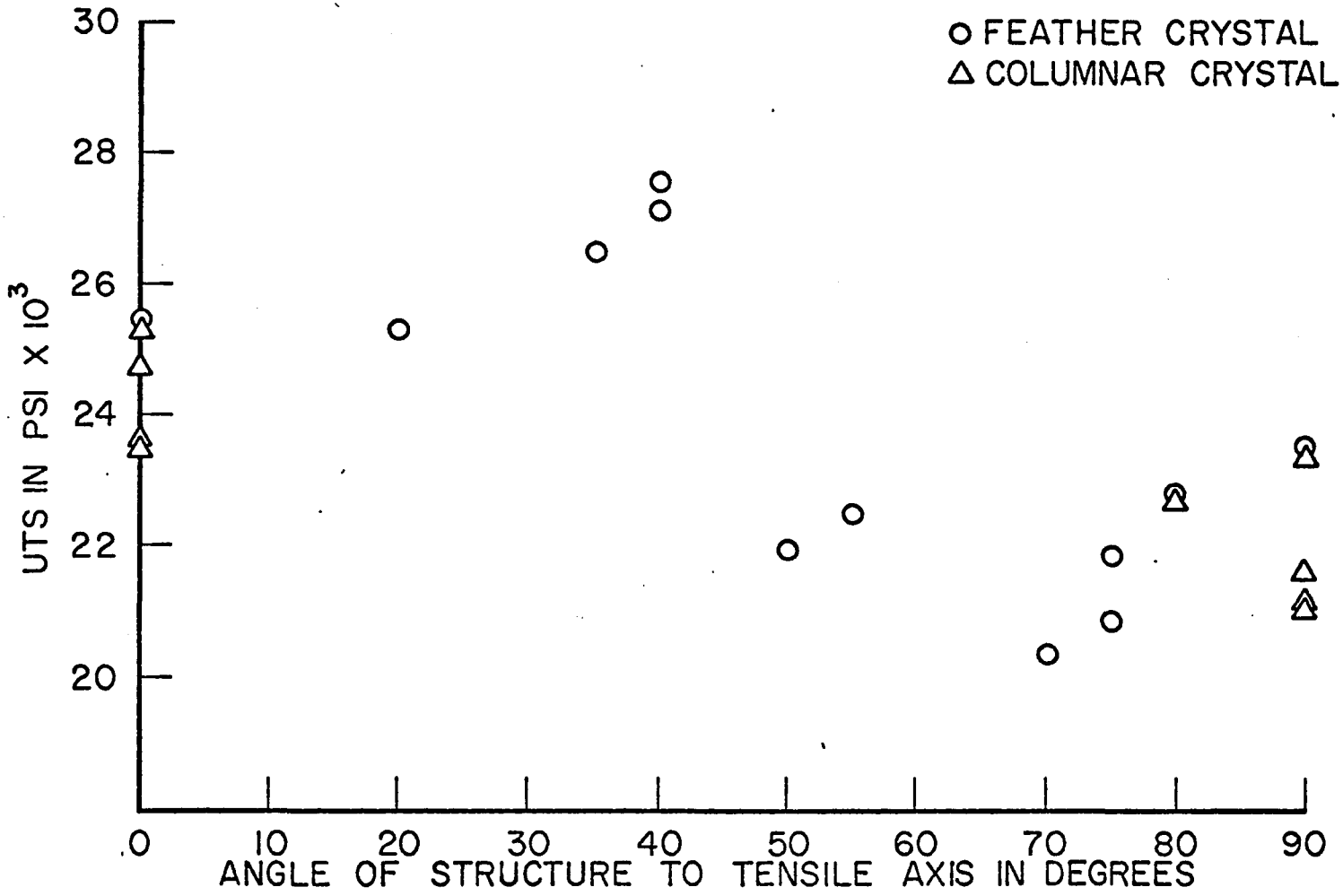

Fig. 37. The Ultimate Tensile Strength of Directionally Cast 356 Alloy vs. the "Structure Angle".

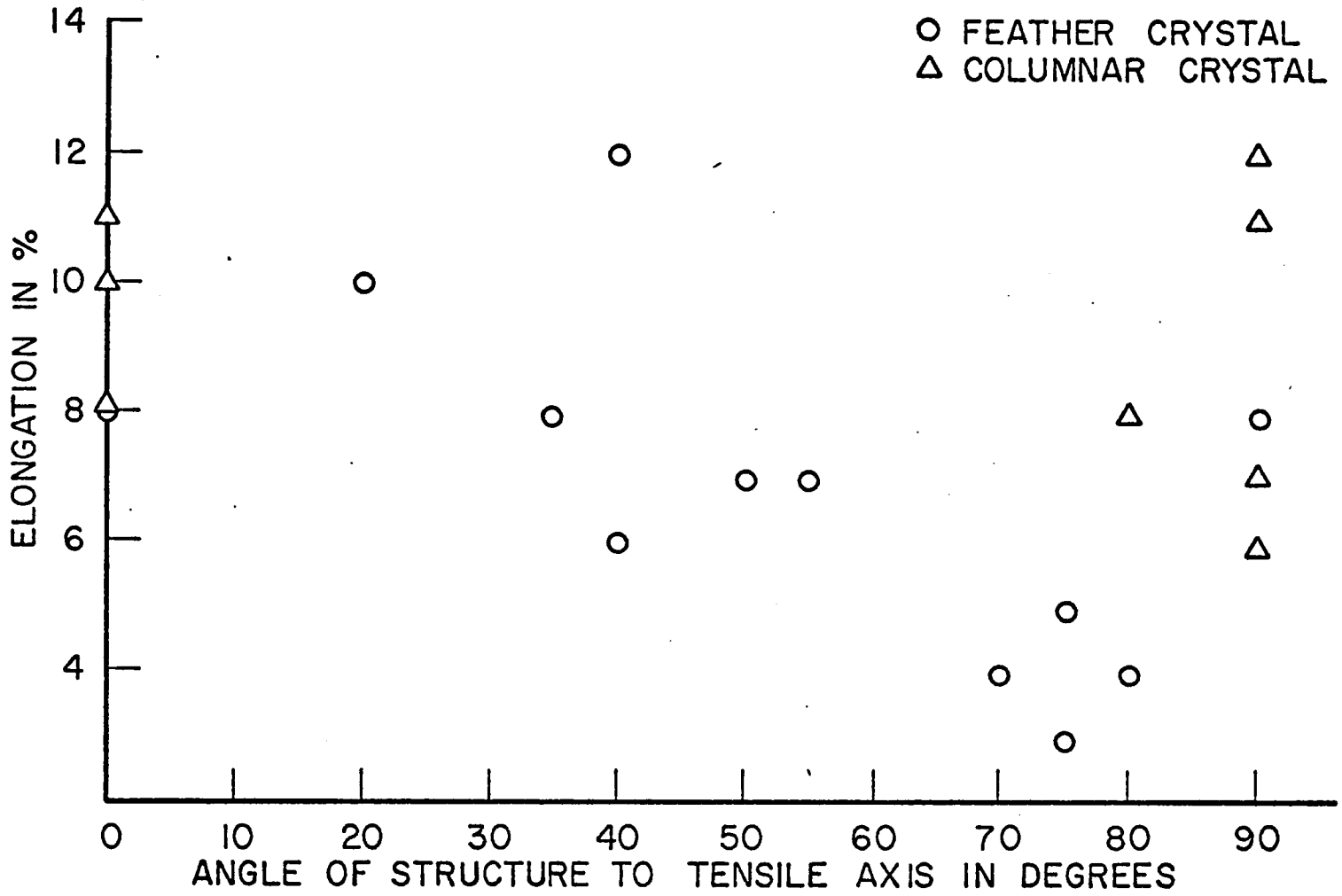

Fig. 38. The Elongation of Directionally Cast 356 Alloy vs. the "Structure Angle".

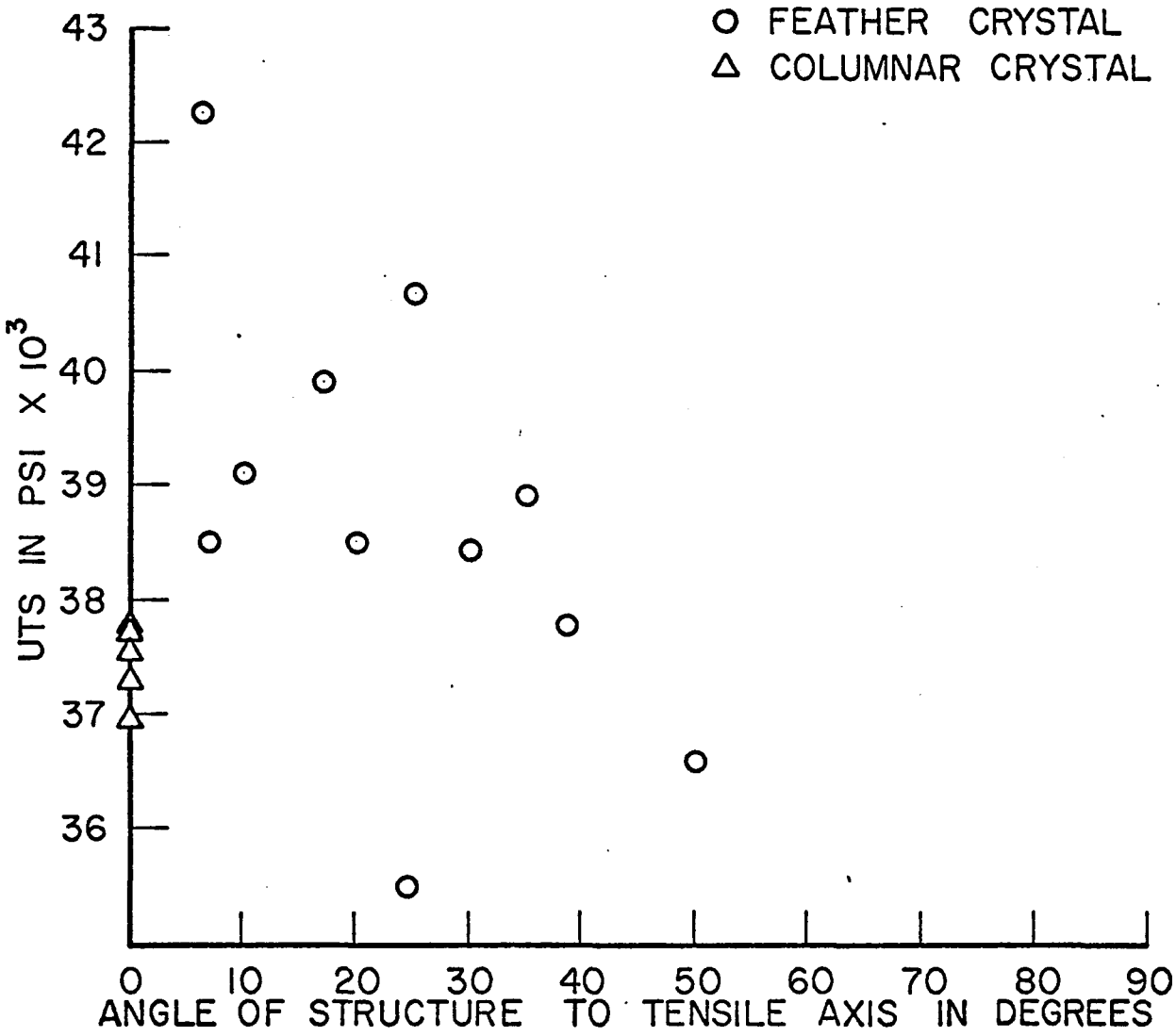

Fig. 39. The Ultimate Tensile Strength of Directionally Cast Tenzalloy vs. the "Structure Angle".

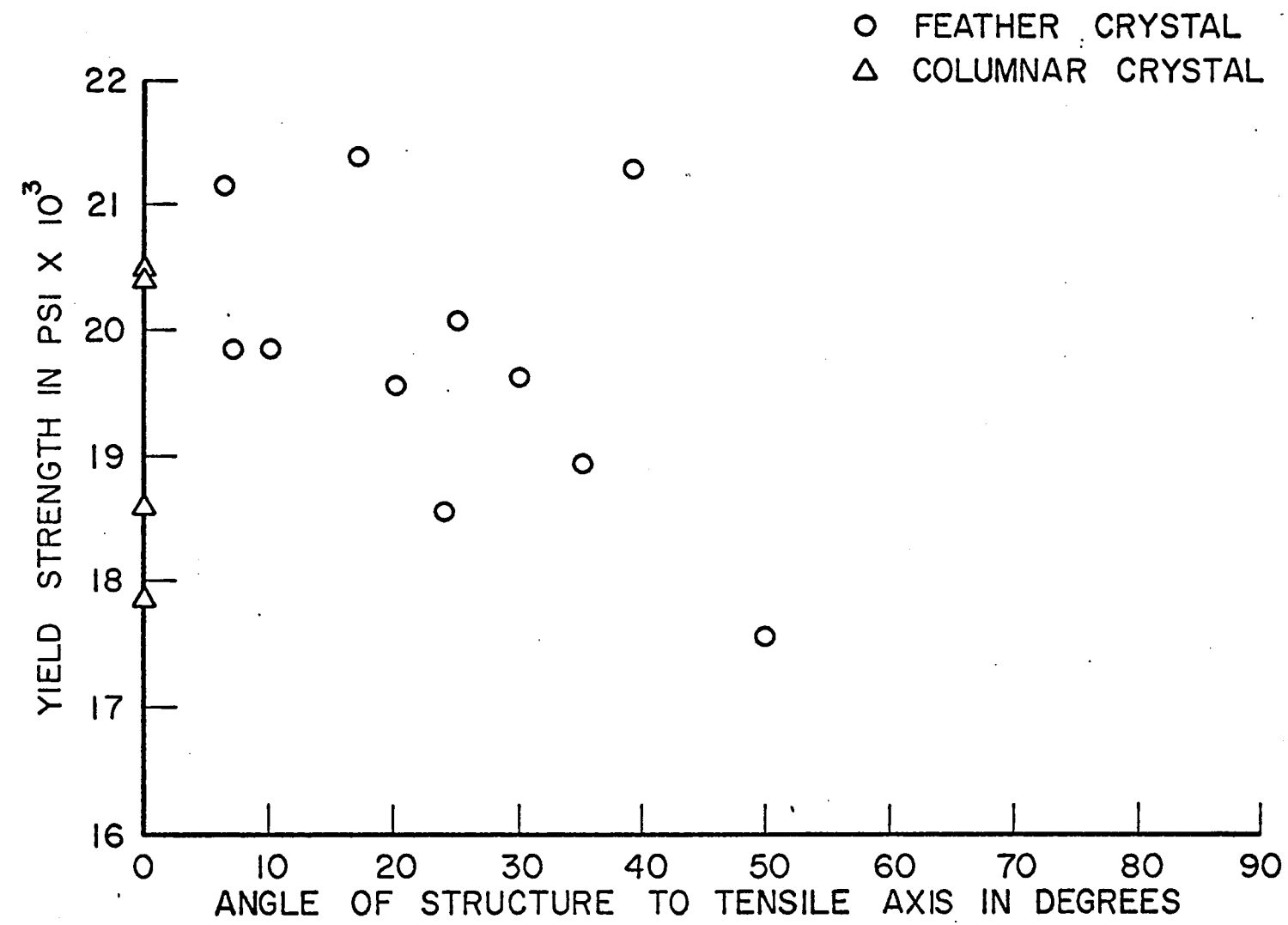

Fig. 40. The Yield Strength of Directionally Cast Tenzalloy vs. the "Structure Angle".

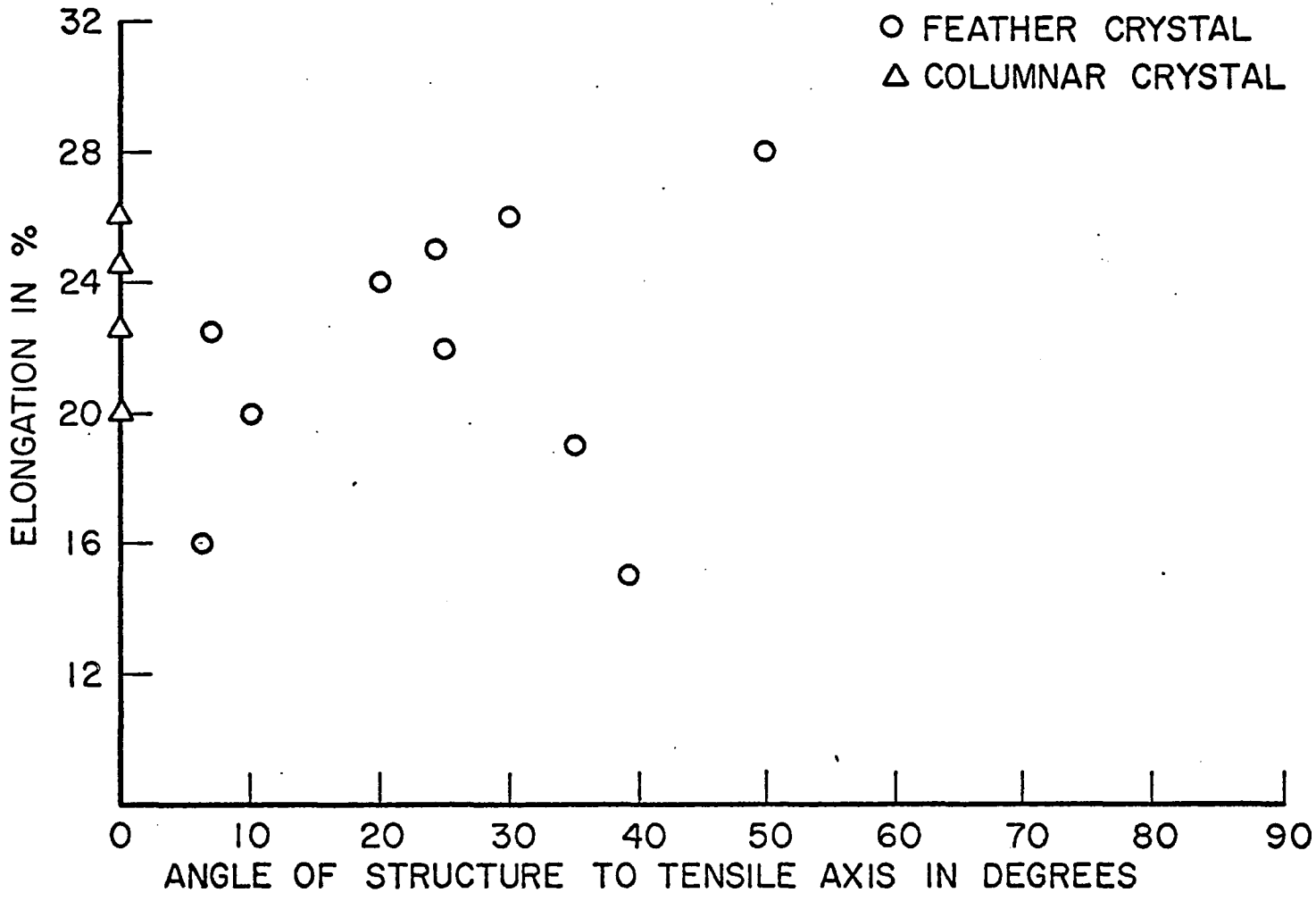

Fig. 41. The Elongation of Directionally Cast Tenzalloy vs. the "Structure Angle".

angle", as mentioned earlier, is the angle measured between the tensile axis of the sample and the traces of the directional grain structure revealed on the surface. A linear regression analysis was performed on the data to describe the relationships. This treatment was an attempt to examine the degree of dependence that the property being evaluated displayed for the "structure angle".

In Fig. 37, the ultimate tensile strength of columnar and feather crystal samples is plotted against the "structure angle". The linear correlation coefficient for this graph was -0.7087. This implies that the data can be described by a straight line within a 90% confidence limit.

The elongation-angle relation is shown in Fig. 38. Both Fig. 37 and Fig. 38 are for the 356 alloy. In this plot, the corelation coefficient was lowered to -0.5925.

The same relationships are plotted for the ultimate tensile strength, yield strength and elongation of Tenzalloy samples in Figs. 39, 40, and 41. The correlation coefficients for these graphs are -0.4985, -0.4853 and -0.2592, respectively. The relation between mechanical properties and the "structure angle" is not well described by a straight line for Tenzalloy. In fact, a curve with a maximum at an angle of 30 degrees to the tensile axis would probably more accurately approximate the data.

The x-ray pinhole diffraction patterns of the Tenzalloy samples of Fig. 28 are presented in Figs. 42, 43, and 44. The sample with the random grain structure gave a spotted ring pattern. The spottiness was caused by the coarse grain size. Both the columnar and feather crystal

Fig. 42. Pinhole Back-Reflection Diffraction Pattern of a Tenzalloy Test Bar with a Random Grain Structure.

Fig. 43. Pinhole Back-Reflection Diffraction Pattern of a Tenzalloy Test Bar with a Columnar Crystal Structure.

Fig. 44. Pinhole Back-Reflection Diffraction Pattern of a Tenzalloy Test Bar with a Feather Crystal Structure.

samples produced diffraction patterns which indicated a high degree of orientation. The occurrence of a single smeared spot made analysis difficult.

The fracture surfaces of the same Tenzalloy samples were examined with an optical microscope. Although the analysis was limited by the depth of field allowable, a good comparison of the surface texture could be made. Low magnification optical micrographs of fracture surfaces are shown in Figs. 45 and 46. The random sample surface is rougher and more irregular than the feather crystal surface which shows clearly the feather lamellae.

A closer inspection of the Tenzalloy fracture surfaces was performed with scanning electron microscopy (SEM). Microfractographs of these surfaces are shown in Figs. 47a through 47i. Interpretation of these photographs was difficult; however, distinguishing features were discernible between the samples.

The major portion of the sample which had a random grain structure is shown in Fig. 47a. There are no indications of cleavage structures and the rounded facets show that ductile failure occurred. Some relatively large microshrinks and dendrite rosettes were observed. Higher magnification views of these two surface observations are shown in Figs. 47b, 47c, and 47d. Not much data on SEM of castings failed in tension was available for the analysis of these photographs.

The fracture surface of the sample which had a columnar crystal structure is shown in Fig. 47e. This surface is more like the typical cup-and-cone ductile failure type than the one observed for the random sample. In a wrought alloy, the central zone of the fracture would

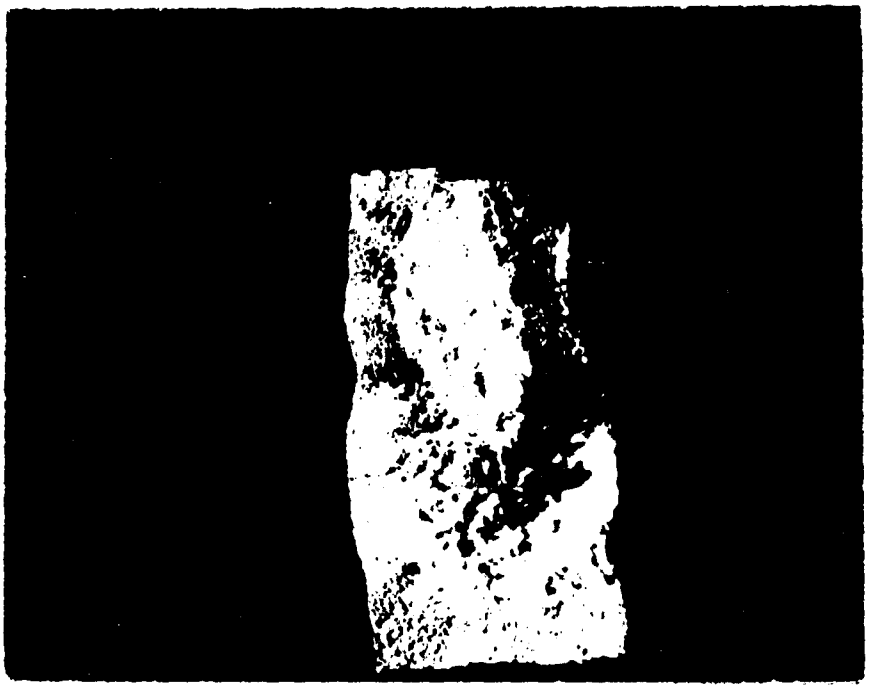

Fig. 45. Optical Fractograph of a Tenzalloy Test Bar with a Random Grain Structure, 5X.

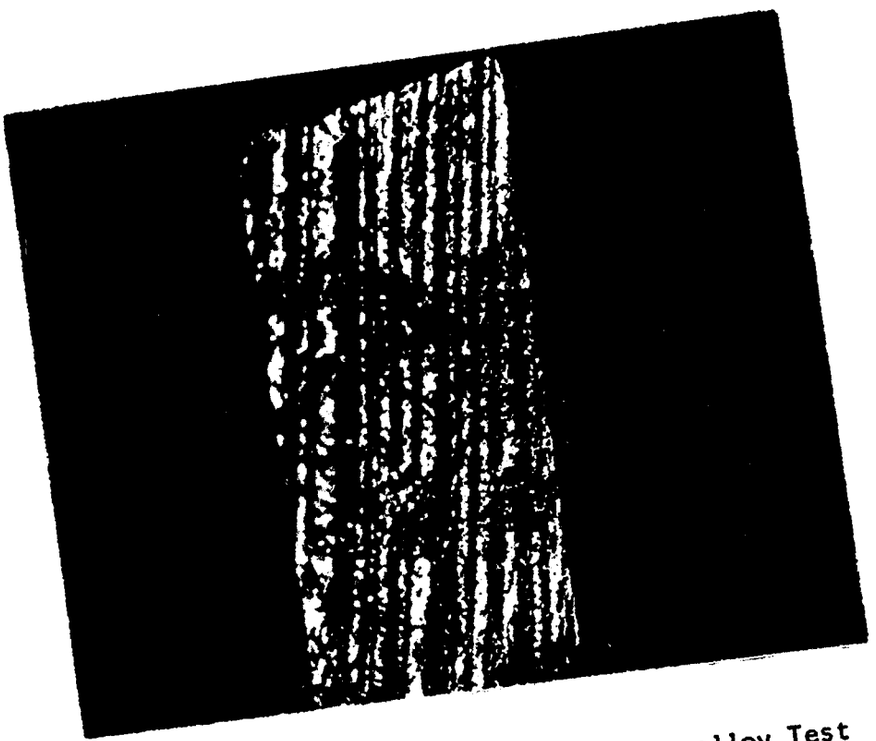

Fig. 46. Optical Fractograph of a Tenzalloy Test Bar with a Feather Crystal Structure, 5X.

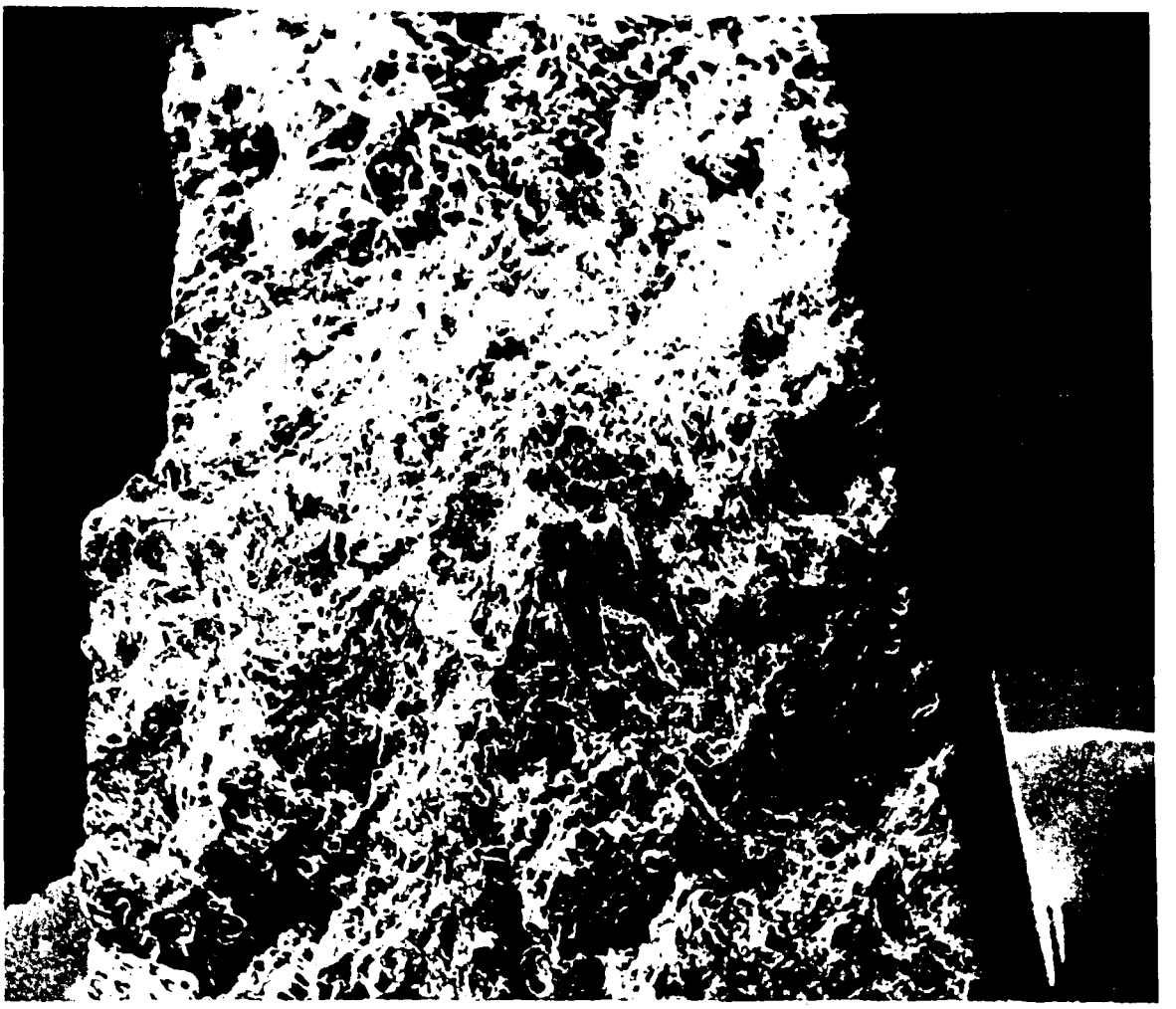

Fig. 47a. Scanning Electron Micrograph of the Fracture Surface of a Tenzalloy Test Bar which had a Random Grain Structure, 25X.

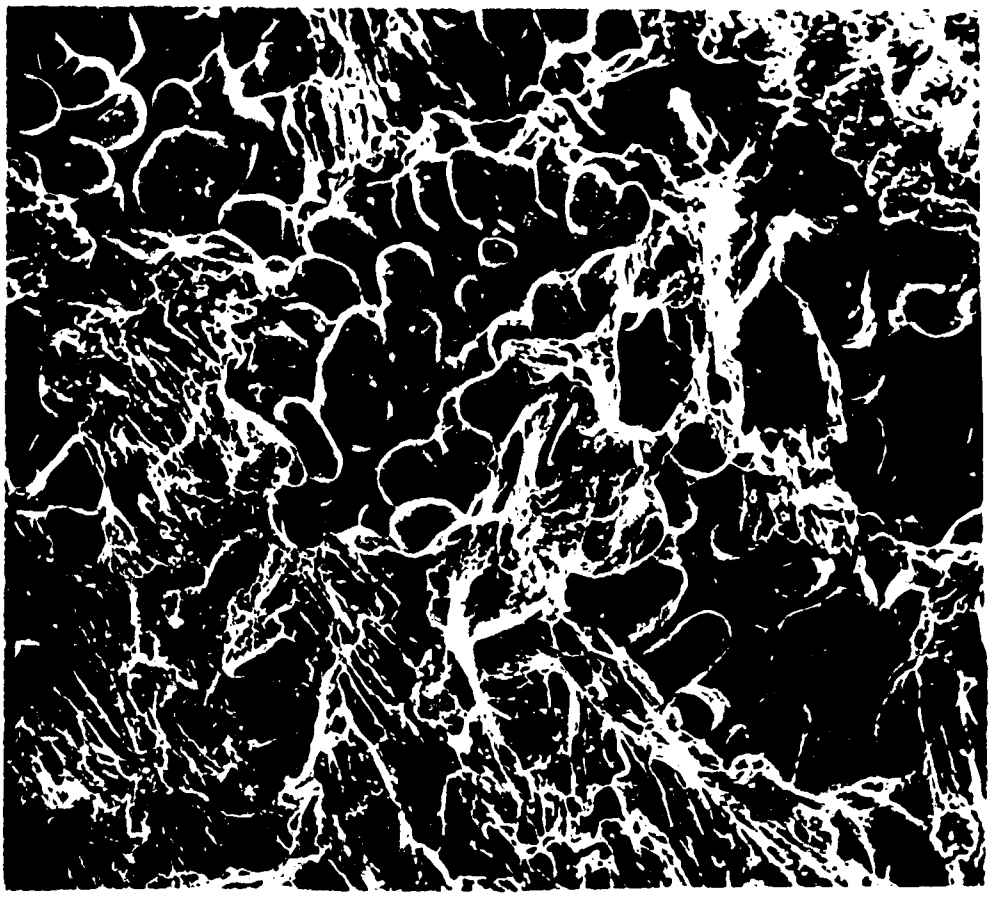

Fig. 47b. Selected Area of Fig. 47a Showing the Structure of the Surface Near a Microshrink, 125X.

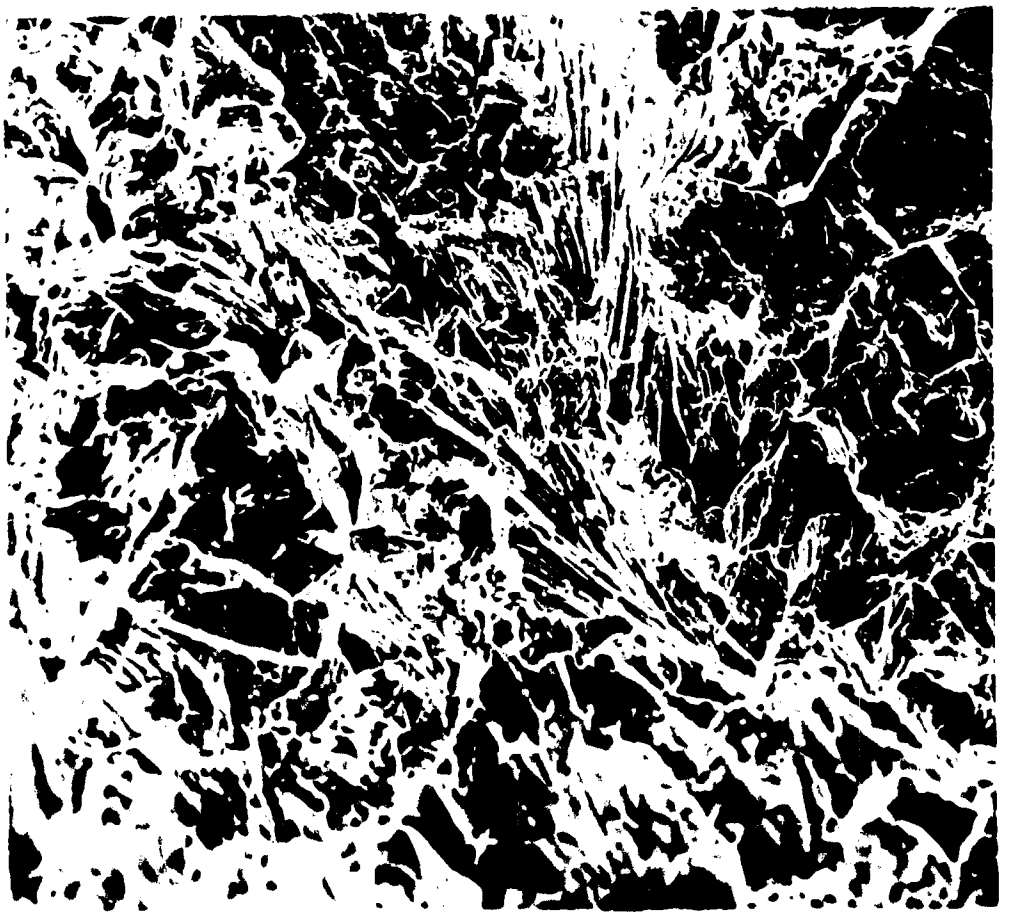

Fig. 47c. SEM Micrograph of the Central Area of Fig. 47a Showing a Dendritic Structure, 128X.

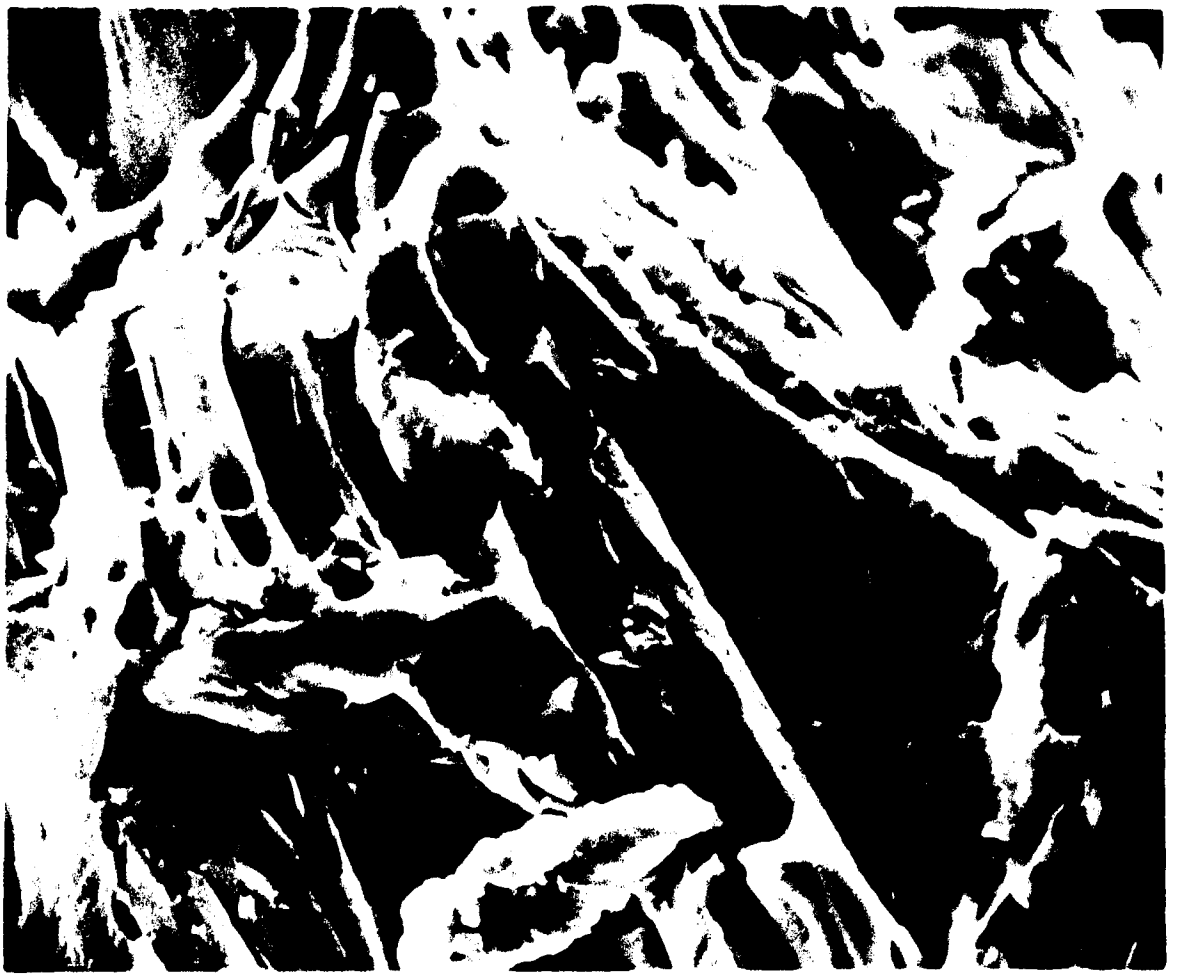

Fig. 47d. The Central Area Dendrites of Fig. 47c Magnified to 1280X.

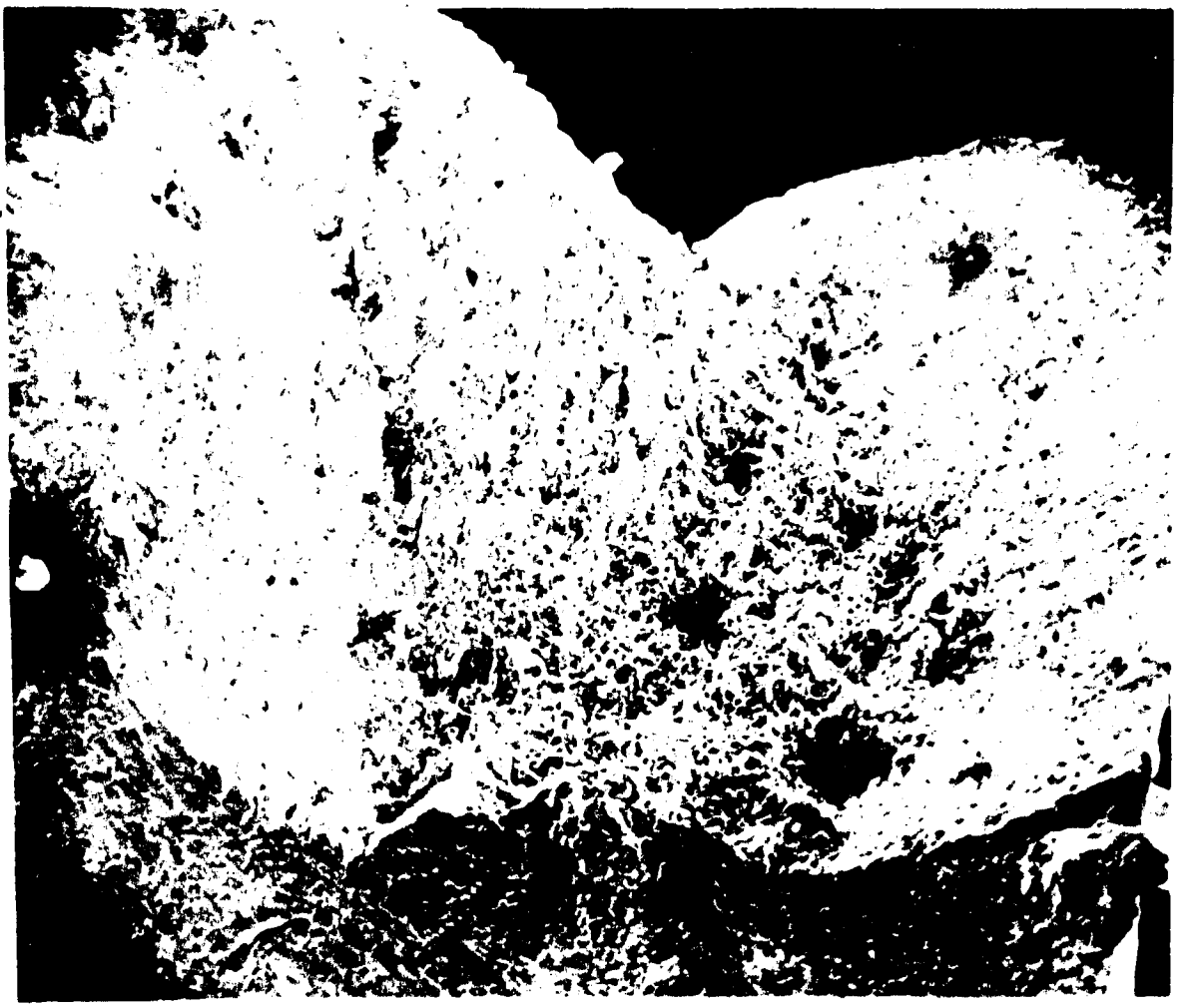

Fig. 47e. Scanning Electron Micrograph of the Fracture Surface of a Tenzalloy Test Bar which had a Columnar Crystal Structure, 25X.

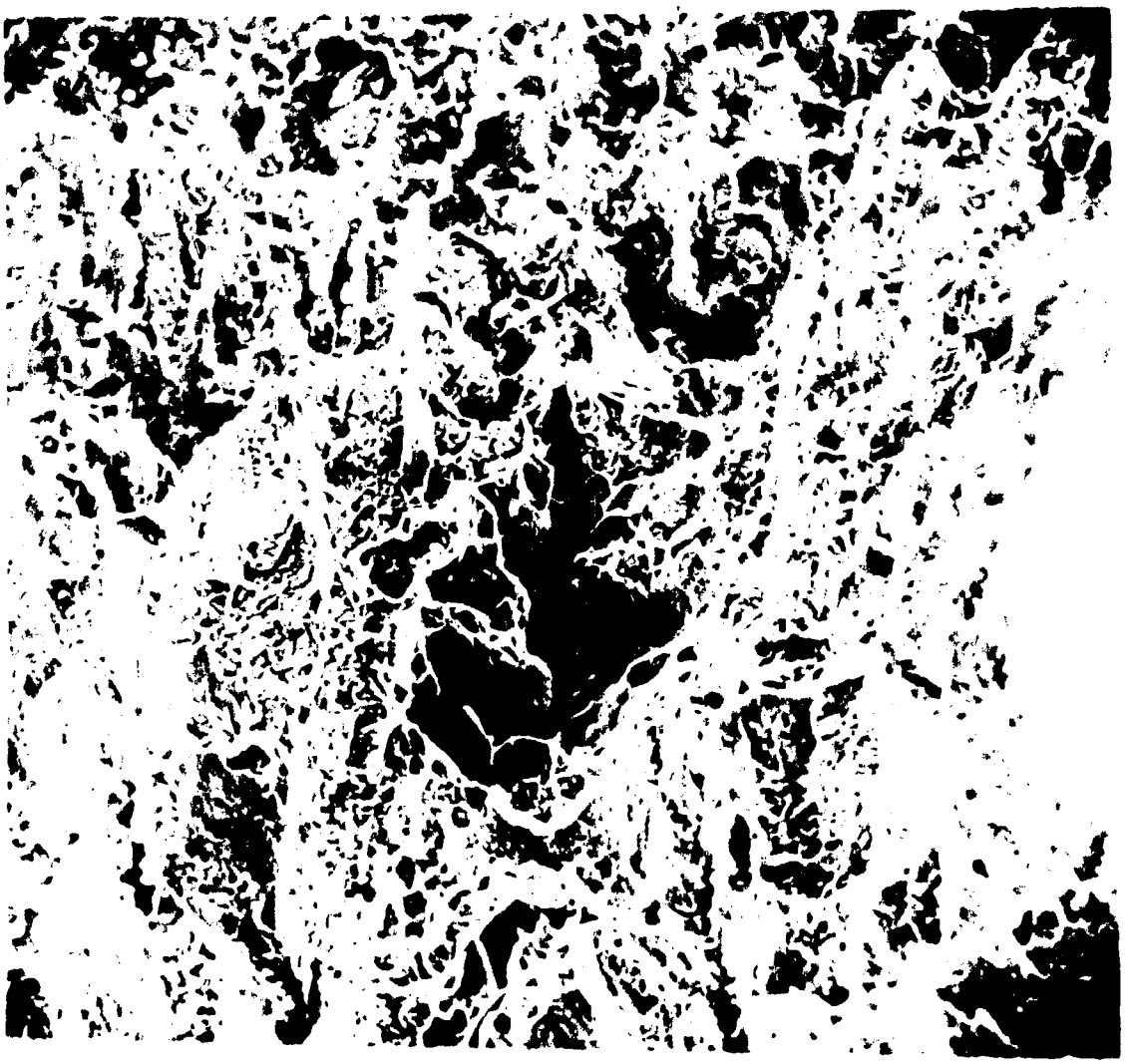

Fig. 47f. Selected Area of Fig. 47e Showing the Structure of the Surface in the Central Region of the Fracture, 140X.

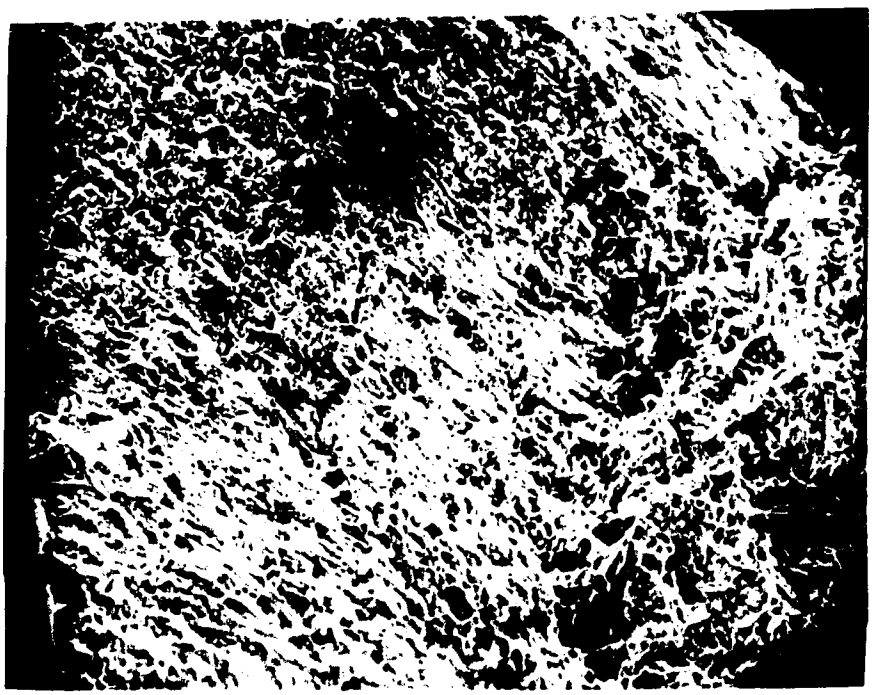

Fig. 47g. SEM Micrograph of the Shear-Lip Region of Fig. 47e, 140X.

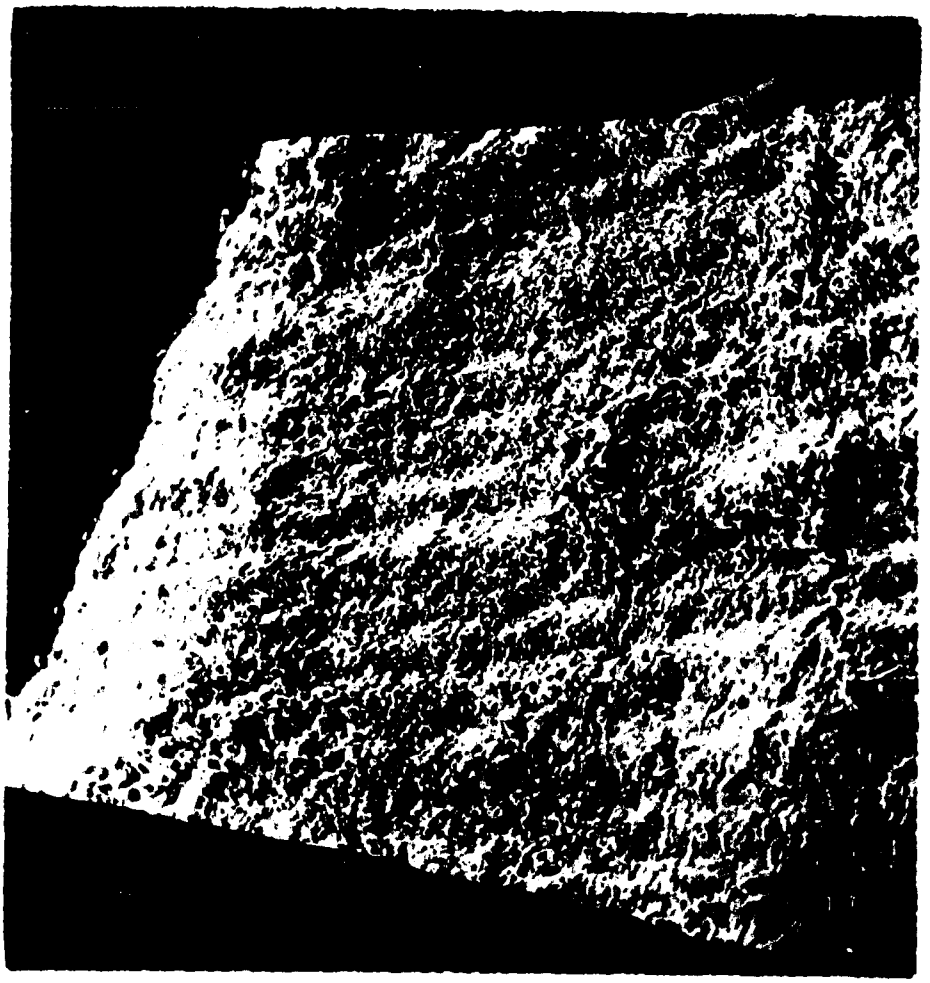

Fig. 47h. Scanning Electron Micrograph of the Fracture Surface of a Tenzalloy Test Bar which had a Feather Crystal Structure, 20X.

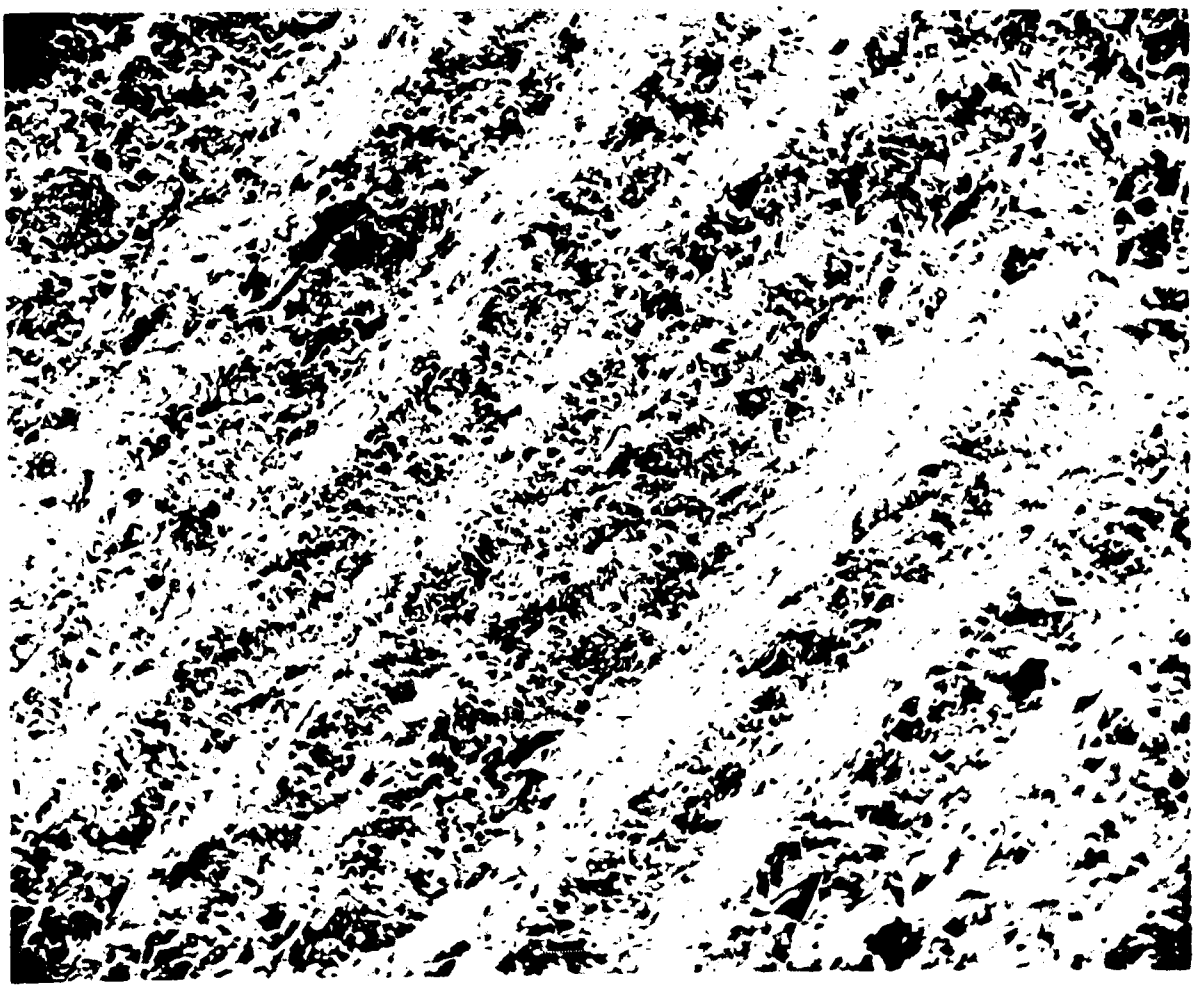

Fig. 47i. Selected Area of Fig. 47h Magnified to 52X.

have shown cleavage surfaces and the shear-lip region would have shown dimples oriented in the direction of failure. These features were not distinctly observed in this sample as seen in Figs. 47f and 47g. Again, castings are more complex in their failure mode than wrought alloys.

The sample with the feather crystal structure had a bright 45° cleavage-type of fracture surface. In Fig. 47h twins are shown in the surface (which was unetched) indicating a step-type of failure. This is further verified in the higher magnification view of Fig. 47i. Unfortunately, the x-ray analysis portion of the microscope was inoperative at the time of the investigation.

Optical Mirror Evaluations

The optical mirror evaluation procedures included casting, grinding, polishing, flatness measuring, and thermal cycling. Two aluminum alloys (356 and Tenzalloy) were cast into discs which were three inches in diameter and 0.5 inches thick. Both randomly oriented and directional structures were made. The pattern used for making the directional castings is shown in Fig. 48. As in the casting of the slabs for the tensile bars, the patterns were centered in a four-inch diameter steel pipe and filled with a slurry of investment (Kerr K-90). Again, the molds were dried, heated to 1290°F overnight and filled with 1400°F superheated metal. Samples with random structures were made in a mold which had a closed cavity and were not poured on the chill block. The lost-wax process was used to make the mold cavity.

An optical flat was made on each mirror blank by surface grinding. Polishing was shown to produce undesirable distortion in the

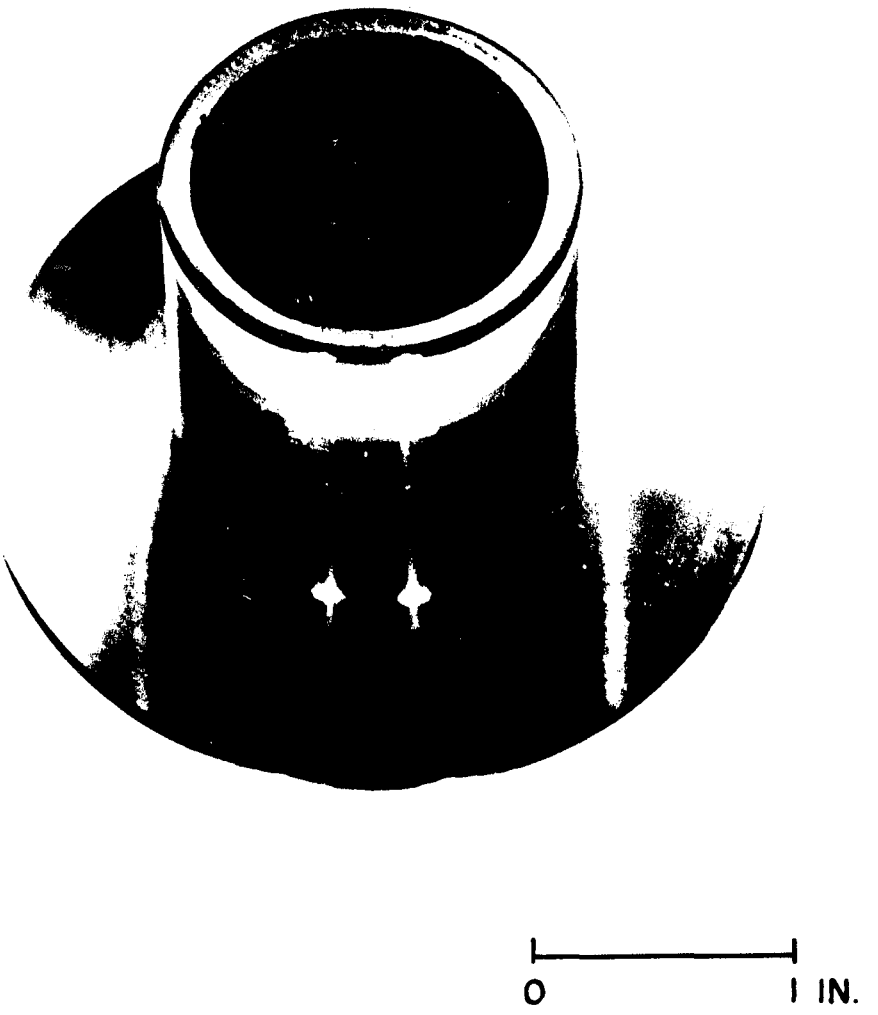

Fig. 48. Pattern used for Casting Mirror Blanks with Directional Structures.

surfaces and was discarded. The flatness of the mirrors was measured with a Fizeau interferometer. The ground blanks were then thermally cycled nine times between -80 and 160°F, being held at each extreme for four hours. After cycling, interferometer readings were taken and the changes in surface flatness were recorded. The difference in surface flatness before and after thermal cycling was interpreted as a measure of the dimensional stability of the cast structures.

Results of the Mirror Evaluations

Seven aluminum alloy mirror blanks were cast and tested for dimensional stability. The results of the interferometer measurements made before and after thermal cycling are presented in Table 6. These values were obtained by drawing a secant to each interferometer ring. The distance from the mid-point of the line to the ring being measured in terms of apparent band width in the photograph was recorded as a measure of surface flatness. Interferograms for Samples 1, 2, 3, and 4 are shown in Fig. 49.

TABLE 6

Effect of Thermal Cycling on Mirror Surface Flatness

Sample	Alloy and Structure	Surface Flatness in Wavelengths	
		Before Cycling	After Cycling
1	356-Random	0.12	0.55 - 1.22
2	356-Random	0.12	0.2 - 0.4
3	356-Random	0.12	0.5 - 1.12
4	356-Directional-long.	0.2	0.2
5	356-Random	0.54	4.0
6	Tenzalloy-Directional-Axial	0.36	0.5
7	Tenzalloy-Directional-long.	0.38	0.25 - 0.5

In the above Table, long. stands for directional grains cast longitudinally in the mirror blank. That is, the grains run across the sample as opposed to running axially.

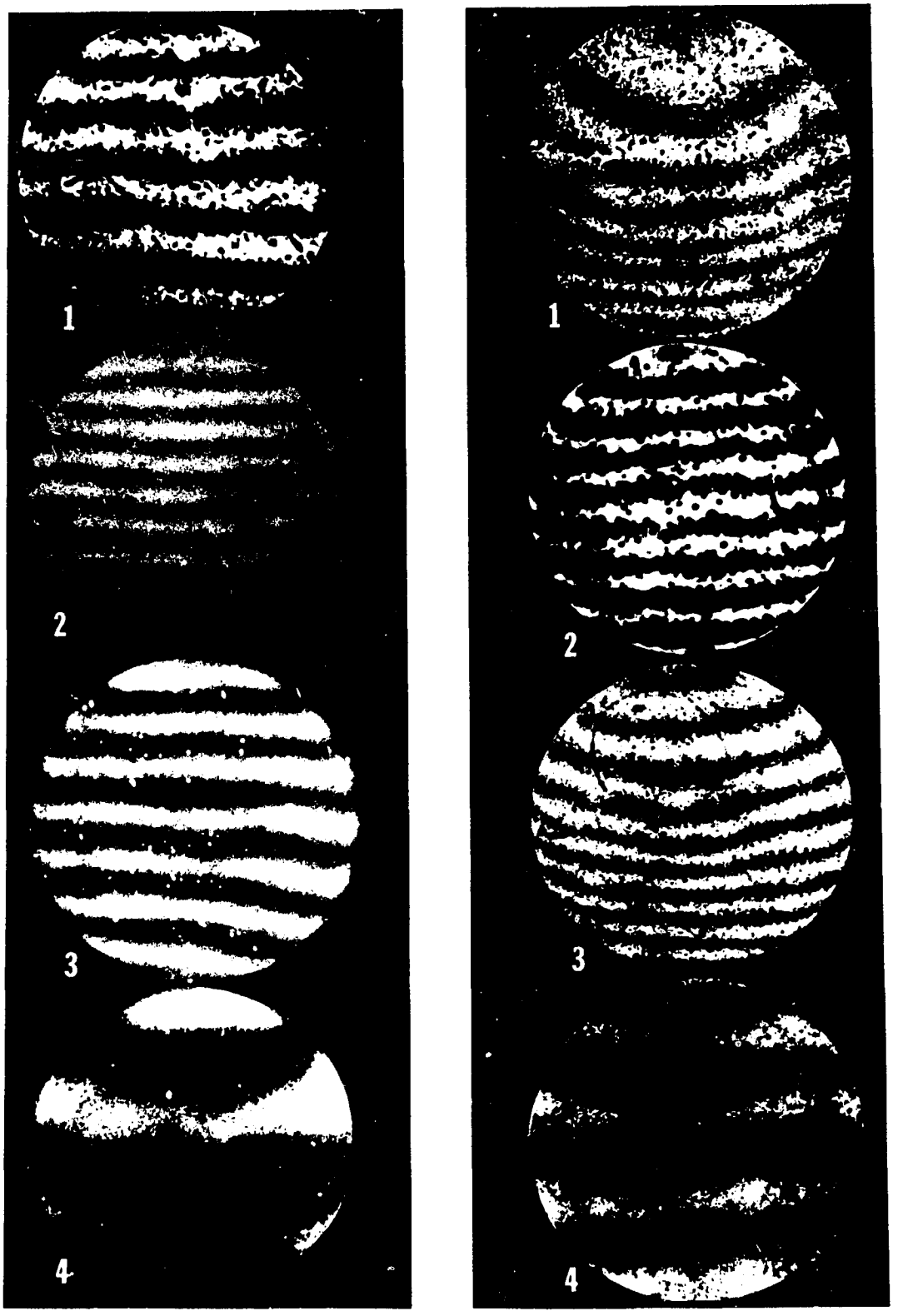

Before Thermal Cycling

After Thermal Cycling

Fig. 49. Interferograms of Mirror Blanks 1, 2, 3, and 4 of Table 5 Before and After Thermal Cycling. Mirror Blank 4 has a Directional Structure.

DISCUSSION OF RESULTS

The results of the experiments to evaluate the properties of unidirectionally solidified aluminum alloys can, in part, be explained in terms of microstructure. The properties of eutectiferous alloys can be qualitatively evaluated on the basis of the proportional amounts of primary crystals, eutectic structure and the physical characteristics of the eutectic (Brick, Gordon, and Phillips, 1965). Strength, ductility and hardness of two-phase alloys are related to the size, distribution and properties of each component.

When a two-phase alloy solidifies from a melt (normally), both components have a coarse structure. If any impurities are present, then the boundaries between components are usually high in concentration of a material which does not add to the strength of the casting. The microstructures of Tenzalloy castings which showed random polycrystals, columnar grains and feather crystals are presented in Figs. 50, 51, and 52, respectively. Both the columnar and feather crystal structures show finer dendrites and a more uniform distribution of the interdendritic eutectic.

Another mechanism of strengthening possessed by directional structures is fiber strengthening as discussed in the Theory section. The fiber component of the aluminum alloys tested is taken to be the interdendritic eutectic. As mentioned earlier, Cahoon and Paxton (1969)

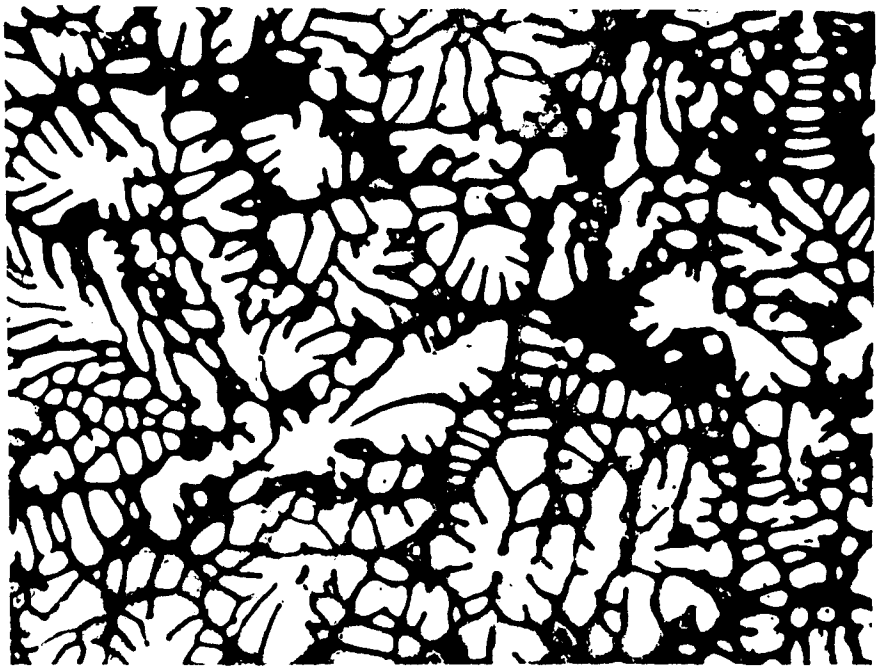

Fig. 50. Typical As-Cast Random Structure of 356 Aluminum at 20X.

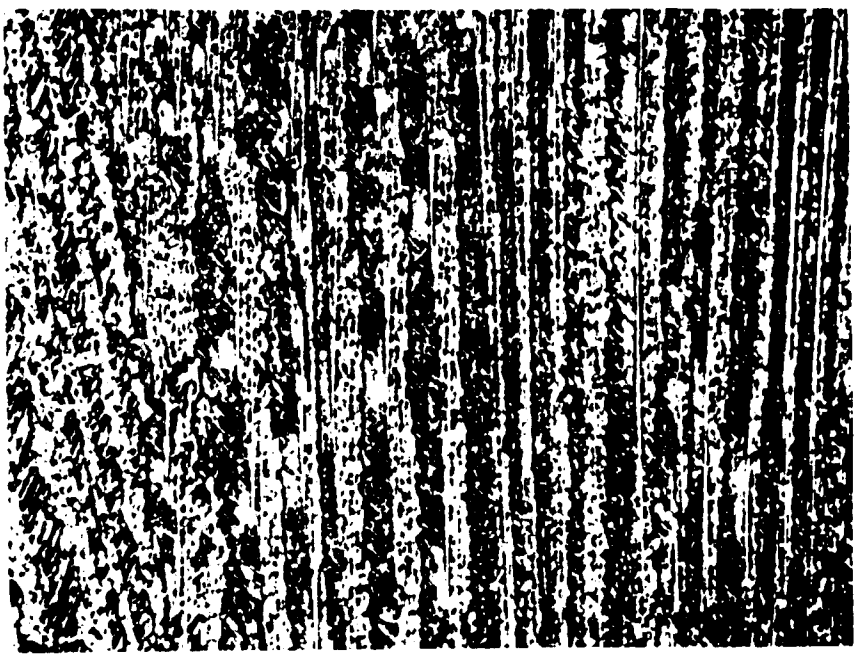

Fig. 51. Typical Microstructure of Columnar Grains in Tenzalloy, 25X.

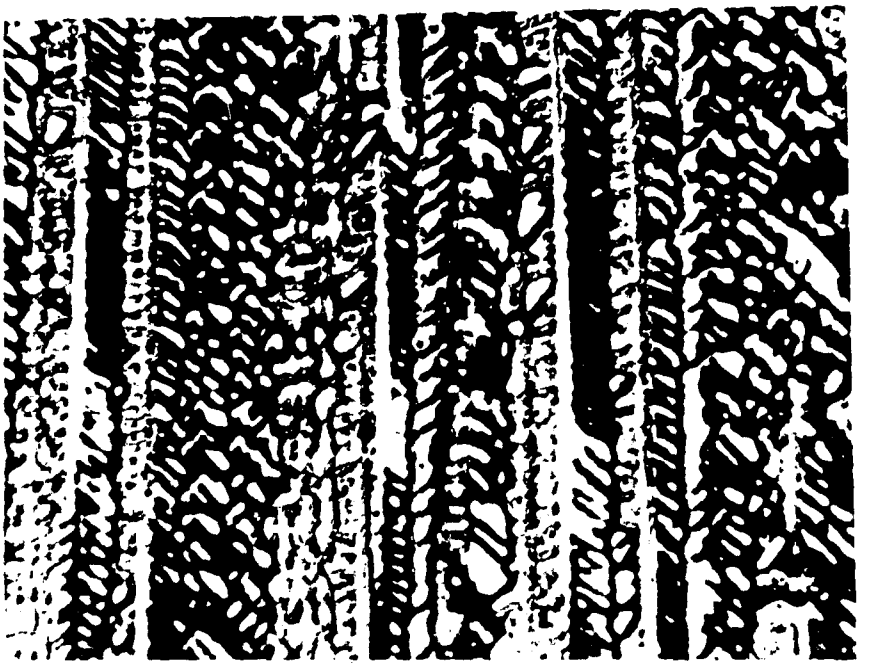

Fig. 52. Typical Tenzalloy Feather Crystal Microstructure, 25X.

evaluated the properties of directionally solidified Al-Mg and Al-Cu alloys with respect to fiber strengthening. Due to the length and shape of the eutectic "fibers", this analysis was not quantitative.

Cahoon and Paxton also investigated the relationship between the volume fraction of interdendritic eutectic and mechanical properties in aluminum alloys. This quantity was varied in their experiments by high temperature solution treatment for various times. It was observed that all mechanical properties improved with decreasing eutectic volume fraction. The change in composition was measured microscopically.

It appears from these observations that the dissolution of a eutectic phase has a large strengthening effect. Since the eutectic was considered to be the fiber component, a decrease in eutectic volume fraction would logically be associated with a decrease in mechanical properties.

Eutectic dissolution is applicable in explaining the results of the heat treatment on the A356 tensile test specimens. In the as-cast condition, the volume fractions of interdendritic eutectic for both random and directional structures were virtually identical. The differences in mechanical properties measured may be totally attributed to fiber strengthening. Upon heat treatment, the amount of interdendritic eutectic was reduced and the structures were refined. The amount of structural refinement observed in the random A356 sample was noticeably more than that in directional A356 as shown in Figs. 53, 54, 55, and 56. The refinement in the random samples was accompanied with a substantial improvement in mechanical properties.

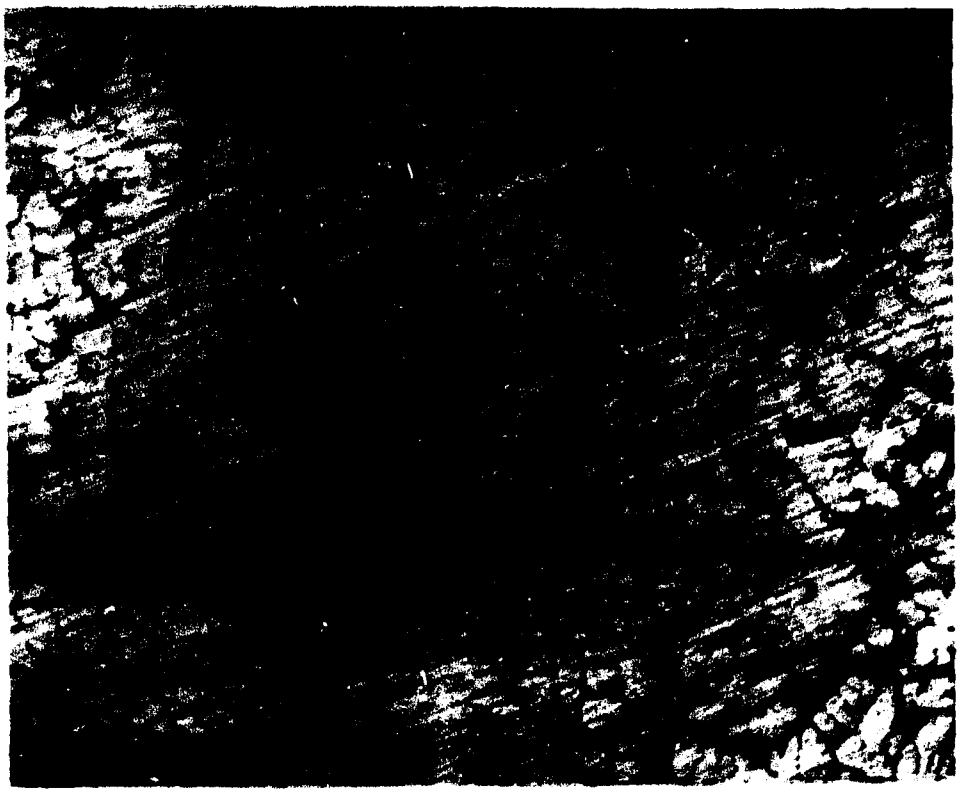

Fig. 53. The As-Cast Microstructure of an A356 Alloy Test Bar which had a Random Grain Structure (Unetched, 20X).

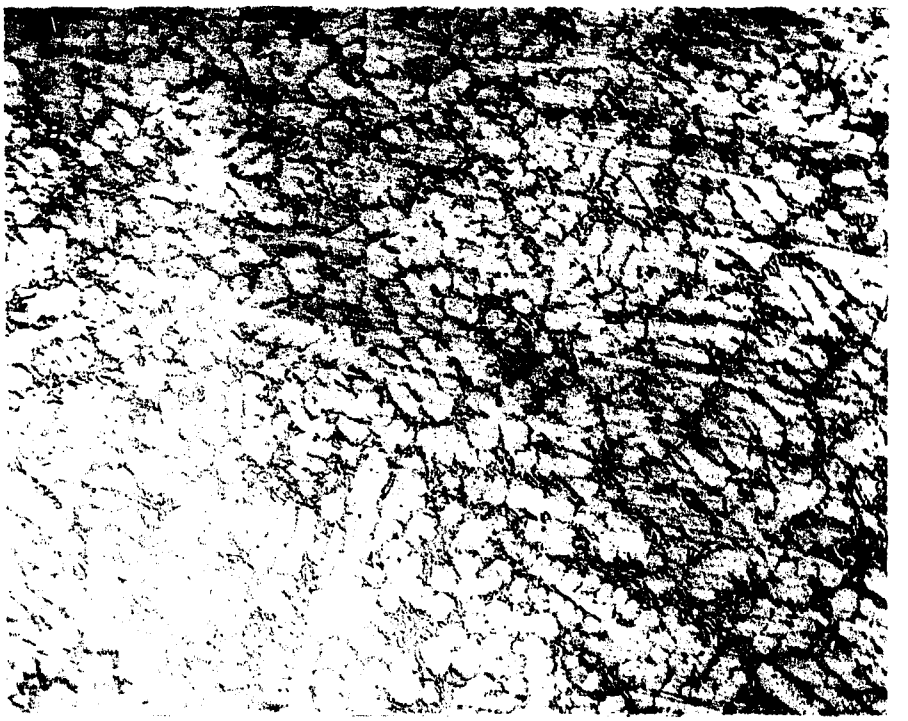

Fig. 54. The Microstructure of an A356 Alloy Test Bar which had a Random Grain Structure after Solution Heat Treatment at 1000°F for 10 hours (Unetched, 20X).

Fig. 55. The As-Cast Microstructure of an A356 Alloy Test Bar which had a Directional Grain Structure (Unetched, 20X).

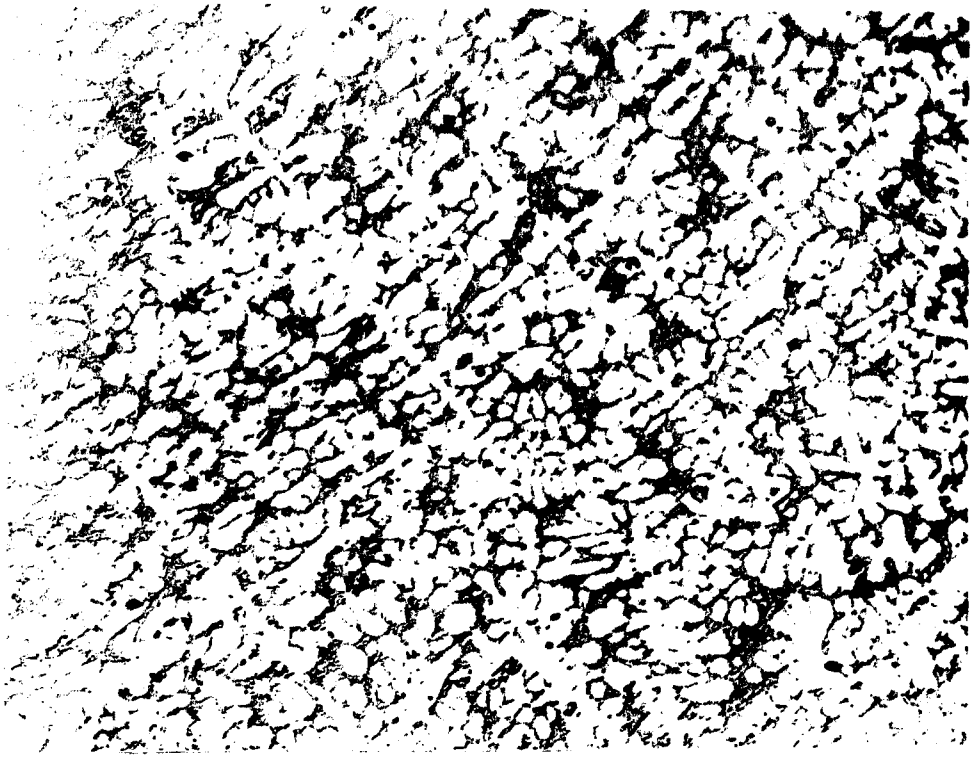

Fig. 56. The Microstructure of an A356 Alloy Test Bar which had a Directional Grain Structure after Solution Heat Treatment at 1000°F for 10 hours (Unetched, 20X).

In the as-cast condition, directional structures were stronger than random polycrystal structures. Samples with feather crystals were generally 34 to 39% stronger and those with columnar crystals were 21 to 35% stronger than samples with a random structure. The values of yield strength were as noticeably different as the data on ultimate strength.

The most impressive and unusual differences in properties observed were in the elongation measurements. Differences of 231 and 226% were noted for specimens with columnar and feather crystals over random samples in Tenzalloy. This variation is visually displayed in the tensile specimens shown in Fig. 57. These are the same Tenzalloy samples which are shown in the un-tested condition in Fig. 28. The columnar and feather crystal samples show considerably greater elongation than the random sample.

Theoretically, spherical particles of eutectic are the ideal shapes for the highest possible composite ductility (Gurland and Plateau, 1963). This postulation obviously does not apply to the columnar and feather crystal structures. A possible corollary to this concept which is more applicable is based on the mean free path between eutectic particles. In the directional structures tested the mean free path between eutectic "fibers" was less than that for a uniform distribution of spherical particles.

In the investigation of the relationship between the "structure angle" and the properties observed, correlations were varied. As shown in Fig. 37 through Fig. 41, the relation of the points to a linear fit varies from very good to not at all.

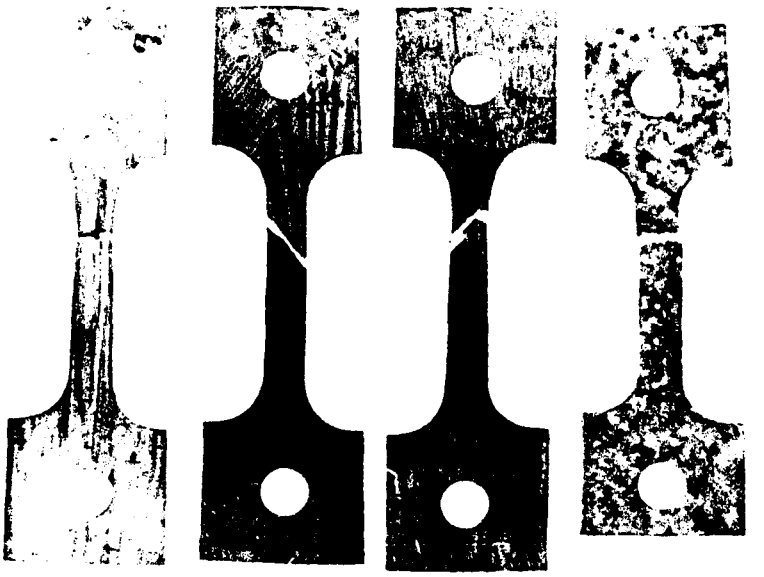

Fig. 57. Tenzalloy Test Bars after Tensile Testing. From the Left: Columnar, Coarse Feather, Fine Feather Crystal and Random Structures.

The improvement in the dimensional stability of optical mirror blanks by directional solidification can be explained in terms of stress relaxation and microyielding. According to a review of the subject (Marschall, Hoskins, and Maringer, 1969), the stresses induced into a metal surface are relaxed during thermal cycling. The metal mirrors of this experiment were ground flat on one side which created an unsymmetric residual-stress distribution. The effect of thermal cycling may be viewed from three standpoints:

a. Severe thermal gradients can generate thermal stresses of sufficient magnitude to cause plastic strains.

b. Differences in thermal-expansion coefficients, either with respect to different crystal directions or with respect to different phases in a multiphase alloy, can lead to internal stresses, even in the absence of severe thermal gradients.

c. Raising the temperature on the top side of the thermal cycle can lead to an increased thermal activation of microdeformation processes.

From the results of the mirror blank evaluations conducted in this experiment, apparently effect b was the most applicable. The directional structures of the alloys investigated, both axial and transverse, were considerably more stable than the random structures. From the rest results, it appears that when the structure of a metal body is highly oriented, the amount of unsymmetric stress induced during thermal cycling is minimized. A rigorous experiment to determine the stresses

involved in thermal cycling with respect to the distribution of phases in the mirror blanks was beyond the scope of this investigation.

CONCLUSIONS AND RECOMMENDATIONS FOR FUTURE WORK

In general, it may be concluded that in the as-cast condition, two-phase aluminum alloys can be unidirectionally solidified into structures which show better mechanical properties than random structures. Feather crystals can be confidently produced in castings by superheating a melt about 250°F and rapidly solidifying in a preheated mold against a chill plate. This investigation showed that the effect of solution heat treatment on as-cast properties was significant. This indicated that dissolution of an eutectic phase was a more effective strengthening mechanism than the fiber strengthening noted for the directional structures.

The most difficult result to explain was the ususually high value of the elongations for as-cast and heat treated directional structures. Possible explanation by the theories of superplasticity was not investigated.

Probably the most significant conclusion was that directionally structured mirror blanks showed better dimensional stability than blanks with a random structure. A program to more thoroughly investigate this phenomenon is currently underway at the University of Arizona Optical Sciences Center. As a future study addition, mirror blanks should be thermally relieved prior to grinding flat.

Some interesting areas to be studied which were revealed by the results of this experiment were:

a. The question of whether or not feather crystals only can occur in aluminum alloys. This structure has not been reported to have been observed in any other alloy system. The question is interesting in that aluminum is not unique as a base material for alloys either in structure or types of phase diagrams.

b. A more thorough investigation of the properties of feather crystals should be performed. A large (three-inch diameter by eight-inch long) ingot should be directionally cast and a complete section of feather crystal lamellae machined out. From this material, true values of feather crystal properties can be obtained.

c. A thorough investigation of the dimensional stability of directionally cast alloys including stress relieving and heat treating should be performed. The results of this type of research may be a significant contribution to optical mirror manufacturing.

GLOSSARY

Alloy A material of metallic properties composed of two or more elements of which at least one is a metal. Alloys usually possess more strength than pure metals.

A356 An aluminum base alloy containing the following ingredients: 6.5-7.5% Si, 0.20% Fe, 0.2% Cu, 0.1% Mn, 0.20-0.40% Mg, 0.10% Zn, 0.20% Ti and 0.15% other. This alloy is predominantly used for investment casting.

Casting The operation of pouring molten metal into a suitable container and allowing it to solidify. The name given to the product of this operation.

Chill A means of rapidly removing heat from a hot mass such as a metal melt.

Constitutional Supercooling The supercooling of a liquid solution by chemically increasing its solute content while keeping its temperature constant. This takes place at the interface of an advancing solid in an alloy where the partition coefficient is less than 1.0.

Eutectic In an alloy system, that particular composition which melts and solidifies at a constant temperature which is lower than the initial solidification temperature of any other composition in the alloy system.

Feather Crystals A name given to the crystal structure observed in some unidirectionally solidified aluminum alloys. Also called growth twinned crystals.

Fizeau Interferometer A device for measuring the flatness of a surface by the use of optically flat glass plates and yellow lighting. Differences in heights on a surface are measured in waves (1 wave = 0.000027 inches).

Growth Twin Crystals See feather crystals.

Heat Treating An operation or series of operations in which a metal in the solid state is taken through stages of heating and cooling to obtain desired properties. In aluminum alloys these steps are called solution treating and aging or precipitation hardening.

KO1 An aluminum alloy made by the Olin Mathieson Co. which has the following composition: 0.01% Si, 0.01% Fe, 4.68% Cu, 0.27% Mn, 0.30% Mg, 0.23% Ti and 0.61% Ag. This alloy forms a total solid solution.

Pinhole Back-Reflection An x-ray analysis method which, when used on polycrystalline materials, is capable of showing degrees of preferred orientation.

Macroscopic Etching The use of chemical reagents on a surface to reveal the major grain structure by orientation contrast. The structure can be categorized as random or directional by direct observation.

Microscopic Etching The use of chemical etchants to attack the metal surface sufficiently to reveal the microstructure (second phases, dendrites, etc.) when viewed at high magnification.

Mold A cavity containing structure in which molten metal can be solidified. This is usually made of a refractory material or a metal of high melting temperature.

Optical Flat A surface on a material which is flat enough such that a reflected image is virtually distortion free.

Partition Coefficient The slope of the liquidus curve for an alloy system. It is the measure of the degree of solute rejection from an advancing solid in unidirectional solidification. At equilibrium and at a specific temperature, $k_o = C_s/C_l$.

Solute The minor constituent of a solution. In an alloy, it is the ingredient other than the base metal or solvent.

Solute Redistribution When solute is rejected from an advancing solid interface, it is redistributed in the remaining liquid mainly by diffusion. The final distribution of solute in a solidified ingot is related to the solidification rate.

Structure Angle The angle measured between the tensile axis of a tensile test bar and the traces of the directional grain structure revealed on the sample surface.

Supercooling The process of lowering the temperature of a melt below the liquidus (freezing) temperature without solidification occurring. In this condition, rapid solid growth rates can occur.

Superheating Heating the molten metal to some significantly higher temperature than its equilibrium melting temperature.

Tenzalloy An aluminum casting alloy produced by the Federated Metals Division of ASARCO. It has the following composition: 0.6% Cu, 7.5% Zn, and 0.4% Mg. It is unique as an alloy which ages at room temperature without solution treating.

Thermal Cycling The process of repeatedly heating and cooling a sample after holding for an adequate soaking period at each thermal extreme. This is a test for the dimensional stability of a precision surface or dimension.

Unidirectional Solidification The process of creating a solid mass from a melt by selective freezing from one location of a mold. When properly performed, a planar solid interface sweeps through the mold.

356 An aluminum casting alloy the composition of which is: 6.5-7.5% Si, 0.5% Fe, 0.20% Cu, 0.10% Mn, 0.20-0.40% Mg, 0.20% Zn, 0.20% Ti and 0.15% other.

REFERENCES

Alcoa Aluminum Handbook, Aluminum Co. of America, Pittsburg, 1962.

Aust, K. T., Krill, F. M. and Morral, F. R., J. Metals, 4, 865, 1952.

Barrett, C. H., and Levenson, L. H., Metals Tech., April, 1940.

Benn, E. and Walker, W. W., Met. Trans, 2, 2735, 1971.

Brick, R. M., Gordon, R. B., and Phillips, A., "Structure and Properties of Alloys", McGraw-Hill, New York, 1965.

Cahn, R. W., "Physical Metallurgy", North Holland, Amsterdam, 1965.

Cahn, R. W., Hillig, W. B. and Sears, G. W., Acta Met., 12, 1421, 1964.

Cahoon, J. R. and Paxton, H. W., Trans. AIME, 245, 1401, 1969.

Chadwick, G. A., "Eutectic Alloy Solidification", Pergamon Press, New York, 1964.

Chalmers, B., "Principles of Solidification", John Wiley and Sons, New York, 1954.

Cibula, M. A., J. Inst. Metals, 76, 321, 1950.

Cibula, M. A. and Ruddle, R. W., J. Inst. Metals, 76, 361, 1949.

Doan, G. E., "Physical Metallurgy", McGraw-Hill, New York, 1953.

Elbaum, C. and Chalmers, B., Can. J. Phys., 33, 196, 1955.

Engles, S., Aluminum, 45, 740, 1969.

Flemmings, M. C., Science and Technology, Dec., 13, 1968.

Flemmings, M. C., Uram, C. Z., and Taylor, H. F., Trans. Am. Foundrymans Soc., 68, 670, 1960.

Graf, L., Z. Metalkunde, 29, 133, 1954.

Gullman, L. and Johansson, L., Paper No. A72-43, AIME Conference, San Francisco, Feb., 1972.

Gurland, J. and Plateau, J., Trans. ASM, 56, 442, 1963.

Herenguel, J., Revue de Metallurgie, 45, 139, 1948.

Hurle, D. T. J., "Mechanism of Growth from the Melt", Pergamon Press, London, 1962.

Jackson, K. A. and Chalmers, B., Can, J. Phys., 34, 473, 1956.

Kelly, A., "Strong Solids", Clarendon Press, Oxford, 1966.

Korolkov, A. M., "Casting Properties of Metals and Alloys", Consultants Bureau Enterprises, New York, 1963.

Marschall, C. W., Hoskins, M. E., and Maringer, R. E., "Continuation of a Study of Stability of Structural Materials for Spacecraft Application", Battelle Memorial Institute, Columbus, Ohio, 1969.

Miyazawa, S., Honma, U., and Oya, S., Report Cast. Lab. Waseda Univ., Tokyo, No. 20, 55, 1969.

Mollard, F. R. and Flemmings, M. C., Trans AIME, 239, 1526, 1967.

Morris, L. R., Caruthers, J. R., Plumtree, A., and Winegard, W. C., Trans. AIME, 236, 1286, 1966.

Nakao, Y., Light Metals, 27, 5, 1957.

Nereo, G. E., Polich, R. F., and Flemmings, M. C., Trans Am. Foundrymans Soc., 73, 1-13, 1965.

Northcott, L., J. Inst. Metals, 45, 205, 1939.

Pfann, W. G., "Zone Melting", John Wiley and Sons, New York, 1957.

Piearcey, B. J., Kear, B. H., and Smashey, R. W., Trans ASM, 60, 634, 1967.

Piearcey, B. J. and Versnyder, F. L., Metals Progress, Nov., 66, 1966.

Plaskett, T. S. and Winegard, W. C., Trans AIME, 51, 222, 1950.

Polich, R. F. and Flemmings, M. C., Trans Am. Foundrymans Soc., 73, 28, 1965.

Roberts-Austen, W. C., Engineering, 63, 223, 1897.

Rosenberg, A., Thesis, Univ. of Toronto, 1956.

Rosenberg, A. and Tiller, W. A., Acta Met., 5, 565, 1957.

Ruddle, R. W. and Mincher, A. L., J. Inst. Metals, 78, 229, 1950.

Rutter, J. W. and Chalmers, B., Can. J. Phys., 31, 15, 1953.

Salkind, M. and Lemkey, F., Int. Science and Tech., March, 52, 1967.

Schipper, M. and Roth, W., Z. Metalkunde, 47, 78, 1956.

Sicha, W. E. and Balhm, R. C., Trans. Am. Foundrymans Soc., 56, 398, 1948.

Tammann, G., "State of Aggregations", D. Von Nostrand, New York, 1925.

Taylor, H. F., Walther, W. D., and Adams, C. M., Trans. Am. Foundrymans Soc., 62, 1954.

Tiller, W. A., Trans. AIME, 224, 448, 1962.

Tiller, W. A. and Rutter, J. W., Can. J. Phys., 34, 96, 1956.

Versnyder, F. L. and Piearcey, B. J., Modern Castings, 52, 68, 1967.

Versnyder, F. L. and Piearcey, B. J., Modern Castings, 55, 10, 1969.

Versnyder, F. L. and Shank, M. E., Matl. Sci. Eng., 6, 213, 1970.

Wagner, R. S., Acta Met., 8, 57, 1960.

Walker, J. L., "Liquid Metals and Solidification", p. 319, American Society for Metals, Cleveland, 1958.

Walker, W. W. and Benn, E., Metallography, 4, 95, 1971a.

Walker, W. W., and Benn, E., Optical Sciences Newsletter, Univ. of Arizona, Vol. 5, No. 2, Aug., 73, 1971b.

Walton, D. and Chalmers, B., Trans. AIME, 215, 447, 1959.

Walton, D., Tiller, W. A., Rutter, J. W., and Winegard, W. C., Trans. AIME, 203, 1023, 1955.

Watanabe, S., Honma, U., and Oya, S., Report Casting Lab. Waseda Univ., Tokyo, No. 20, 45, 1969.

Webster, G. A. and Piearcey, B. J., Trans. ASM, 59, 847, 1966.

Wineberg, F. and Chalmers, B., Can. J. Phys., 29, 382, 1951.

Wineberg, F. and Chalmers, B., Trans. ASM, 46, 1953.

Winegard, W. C., "An Introduction to the Solidification of Metals", The Institute of Metals, London, 1964.

Wojciechowski, S. and Chalmers, B., Trans. AIME, 242, 690, 1968.

Wojciechowski, S. and Wallis, L., Nukleonika, 14, 659, 1969.